

extract from the OR6 or ORL8 cells treated with 50 μ M of RBV for 8 hours. HPLC analysis was performed as described previously.¹⁵

RNA Interference. Small interfering RNA (siRNA) duplexes targeting the coding regions of human ADK (catalog no.: M-009687-01; Dharmacon, Inc., Lafayette, CO) were chemically synthesized. A nontargeting siRNA duplex (catalog no.: D-001206-13; Dharmacon) was also used as a control. ORL8 cells were transfected with the indicated siRNA duplexes using Oligofectamine (Invitrogen, Carlsbad, CA).¹⁰

Ectopic Expression of ADK. The methods of plasmid construction for ectopic expression of ADK and retroviral infection using the constructed plasmids are described in the Supporting Materials.

Plasmid Construction and Internal Ribosome Entry Site Activity Assay. The method of plasmid construction for internal ribosome entry site (IRES) activity assay is described in the Supporting Materials. The dual luciferase reporter assay for IRES activity was performed by the method described previously.¹⁴

Statistical Analysis. Data are presented as mean \pm standard deviation. The Student unpaired *t* test was performed for statistical analysis between the two groups, and the difference was considered significant at $P < 0.05$.

Results

High Expression Level of ADK in ORL8 Cells. To identify the host factor responsible for the difference in RBV responses between Li23-derived ORL8 and HuH-7-derived OR6 cells, we first recompiled the previous data from complementary DNA (cDNA) microarrays using Li23 and HuH-7 cells. Although we assigned 17 genes that showed dramatic differences in expression between Li23 and HuH-7 cells,¹² none of these genes were considered to be involved in the response to RBV. Expression of IMPDH1 (NM_000883) and IMPDH2 (NM_000884), which were involved in the anti-HCV mechanism of RBV,^{8,10} was also at a similar level between Li23 and HuH-7 cells or between cured ORL8 (ORL8c) and cured OR6 (OR6c) cells (Supporting Table 2).

We next attempted to verify the process of GTP reduction that is expected to occur after RBV is incorporated into cells. To this end, we performed a quantitative HPLC analysis using the extract from the OR6 or ORL8 cells treated with 50 μ M of RBV for 8 hours, which is the working time of RBV against HCV RNA replication.¹⁰ Amounts of IMP and GTP were calculated from the peak area obtained by HPLC

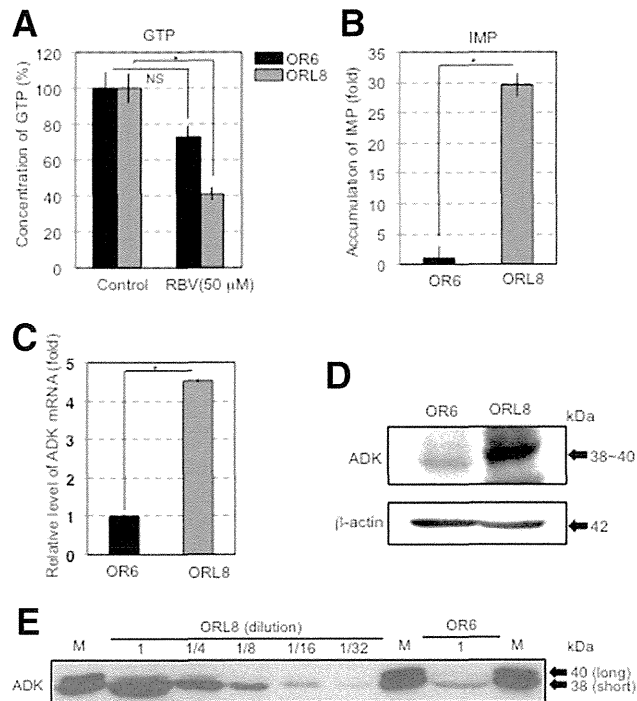


Fig. 1. Expression level of ADK in ORL8 cells was higher than that in OR6 cells. (A) Signal of GTP obtained by HPLC analysis using nts extracted from RBV-treated cells was quantified. (B) Signal of IMP obtained by HPLC analysis using nts extracted from RBV-treated cells was quantified. (C) Expression level of ADK mRNA in ORL8 cells was compared with that in OR6 cells by quantitative RT-PCR analysis. (D) Level of ADK in ORL8 cells was compared with that in OR6 cells by western blotting analysis. (E) ORL8 cell extract was diluted and then western blotting analysis was performed for the detection of ADK. Two isoforms of ADK (40 and 38 kDa) were loaded as molecular markers. Experiments (A-C) were performed in triplicate. * $P < 0.05$; NS, not significant.

analysis. Volume of cells was calculated from the mean diameter of cells, and we found 10^6 cells to be equivalent to 1.1 mm^3 . We assumed that the extracted nucleotides (nts) were uniformly distributed in the cell aqueous volume. As expected, the level of intracellular GTP in ORL8 cells showed a significant (60%) reduction, whereas that in OR6 cells showed only a 27% reduction (Fig. 1A and Supporting Fig. 1A-D). These results support our previous finding that the inhibitory effect of RBV on HCV RNA replication in ORL8 cells is stronger than that in OR6 cells.¹⁰

In addition, we noticed an unexpected phenomenon: A substantial accumulation of IMP occurred as the result of IMPDH inhibition in ORL8 cells, but not in OR6 cells. The IMP level in ORL8 cells became approximately 30 times higher than that in OR6 cells (Fig. 1B and Supporting Fig. 1A-D). However, no additive effect of inosine (up to 100 μ M) on HCV RNA replication in ORL8 cells was observed (Supporting Fig. 2).

It has been reported that RBV is metabolized *in vivo* through RBV 5'-monophosphate (RMP), a

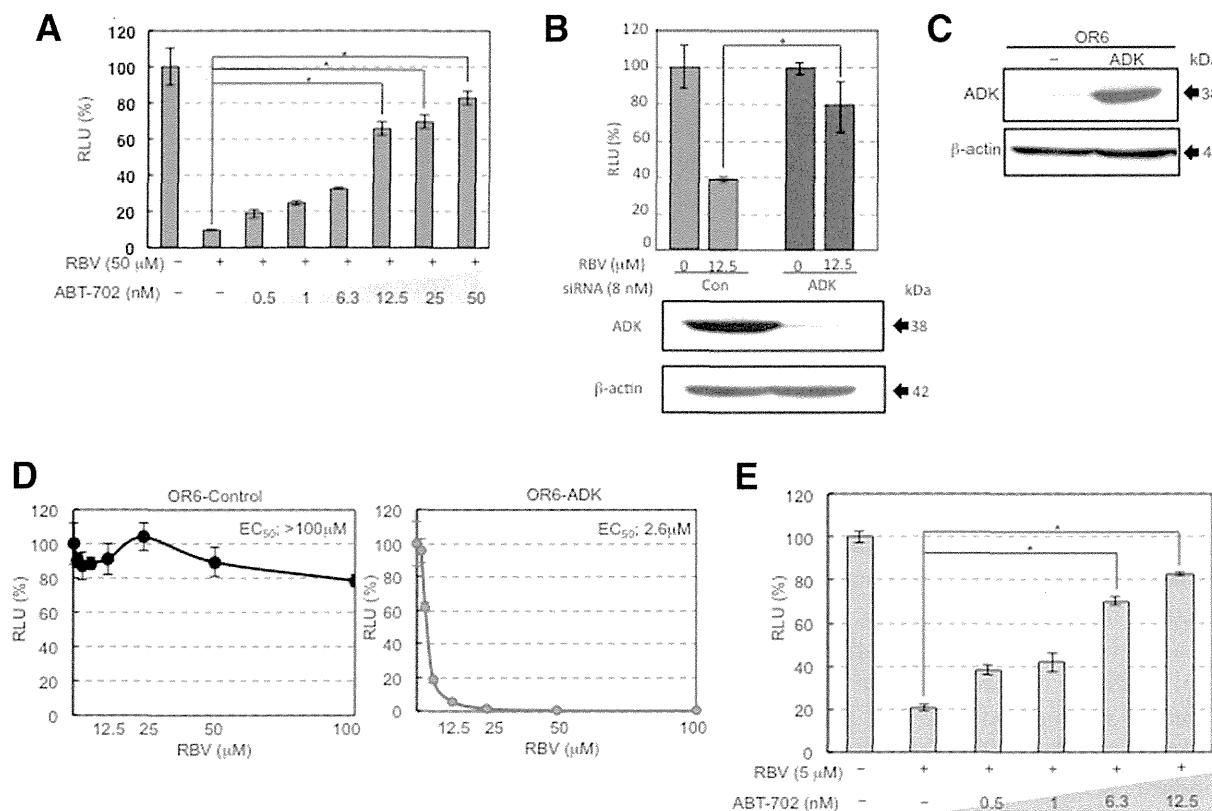


Fig. 2. ADK is a determining host factor for the anti-HCV activity of RBV. (A) ORL8 cells were cotreated with RBV (50 μ M) and ABT-702 (nM) for 72 hours, after which an RL assay was performed. Relative luciferase activity (RLU) (%) calculated at each time point, when the level of luciferase activity in nontreated cells was assigned to be 100%, is shown. (B) ORL8 cells were transfected with 8 nM of siRNA targeting ADK. After 72 hours, expression levels of ADK were monitored by western blotting analysis (lower panel). ADK-knockdown ORL8 cells were treated with 12.5 μ M of RBV for 72 hours, after which an RL assay was performed, as described in (A, upper panel). (C) Expression level of ADK in OR6-ADK cells was monitored by western blotting analysis. (D) OR6-ADK cells were treated with RBV for 72 hours and then an RL assay was performed as described in (A). (E) OR6-ADK cells were cotreated with RBV (5 μ M) and ABT-702 (nM) for 72 hours and then an RL assay was performed, as described in (A). Experiments (A, B, D, and E) were performed in triplicate. * $P < 0.05$.

competitive inhibitor of IMPDH, by ADK.¹⁶ Based on our findings, we expected that ADK activity might be able to control the anti-HCV activity of RBV. Indeed, microarray analysis revealed that the actual expression levels of ADK were 764 and 2,840 in OR6c and ORL8c cells, respectively. Quantitative RT-PCR analysis also showed that the mRNA level of ADK in ORL8 cells was 4.5 times higher than that in OR6 cells (Fig. 1C). Furthermore, we found that the protein level of ADK in ORL8 cells was much higher than that in OR6 cells (Fig. 1D).

On the other hand, it is known that ADK has two major isoforms: ADK-long (NM_006721) localized in the nucleus and ADK-short (NM_001123) localized in the cytoplasm.¹⁷ ADK-long differs in the 5' UTR and initiates translation at an alternative start codon, compared to ADK-short. ADK-long is 17 amino acids longer than ADK-short. We prepared ORL8 cells stably overexpressing ORL8-derived ADK-long or ADK-short using a retroviral gene transfer system and examined its

mobility in western blotting analysis. Fortunately, two isoforms were discriminable as 40 (ADK-long) and 38 kDa (ADK-short) (Fig. 1E). Using these isoforms as molecular markers, we performed semiquantitative western blotting analysis by the sample dilution method. The results revealed that the expression level of ADK-short in ORL8 cells was approximately 16 times higher than that in OR6 cells, and that ADK-long was little expressed in both cells (Fig. 1E). From these results, we assumed that the differences in ADK expression were involved in the dramatic differences in RBV sensitivity between the two cell lines. To address this assumption, we focused on the ADK-short in the following study; hereafter, ADK-short is designated as ADK.

ADK Is a Host Factor Determining the Anti-HCV Activity of RBV. To evaluate the hypothesis that ADK controls the anti-HCV activity of RBV, we first examined the effect of ABT-702, an ADK inhibitor, on the anti-HCV activity of RBV. The results revealed that ABT-702 cancelled the activity of RBV in ORL8

cells in a dose-dependent manner (Fig. 2A). Furthermore, we demonstrated that the activity of RBV was cancelled in ADK-knockdown ORL8 cells (Fig. 2B). These results suggest that the inhibition of ADK in ORL8 cells converts them from an RBV-sensitive phenotype to an RBV-resistant phenotype.

To directly demonstrate the involvement of ADK, we first prepared OR6 cells stably expressing ADK (OR6-ADK) (Fig. 2C). We were able to demonstrate that the OR6-ADK cells were dramatically converted from an RBV-resistant phenotype with an EC_{50} value of more than 100 μ M to an RBV-sensitive phenotype with an EC_{50} value of 2.6 μ M (Fig. 2D). We next examined whether or not the GTP reduction or IMP accumulation observed in ORL8 cells treated with RBV (Fig. 1A,B) occurs in OR6-ADK cells. The results revealed that the GTP reduction and IMP accumulation in RBV-treated OR6-ADK cells were more pronounced than in RBV-treated ORL8 cells (Supporting Fig. 3A,B). Because OR6 is a clonal cell line harboring genome-length HCV RNA, we used a polyclonal cell line (sOR) harboring HCV replicon RNA⁹ to prepare sOR-ADK cells stably expressing ADK (Supporting Fig. 3C) and examined their sensitivity to RBV. sOR-ADK cells were also dramatically converted from an RBV-resistant phenotype with an EC_{50} value of more than 100 μ M to an RBV-sensitive phenotype with an EC_{50} value of 6.0 μ M (Supporting Fig. 3D). In addition, ORL8-ADK cells stably overexpressing ADK also showed EC_{50} values ranging from 13.2 to 1.2 μ M (Supporting Fig. 3E). Furthermore, we demonstrated that the anti-HCV activity detected in OR6-ADK cells was also cancelled by ABT-702 treatment in a dose-dependent manner (Fig. 2E). Considering these results together, we conclude that ADK is a key determinant for the anti-HCV activity of RBV.

The Suppression of ADK Expression in OR6 Cells Was Not the Result of Genetic Variations or Epigenetic Alterations in the ADK Gene Promoter. To clarify the mechanism underlying the difference in ADK expression between OR6 and ORL8 cells, we first examined the nt sequences of up to several kb upstream from the transcription start point estimated from NM_001123 (31-OCT-2010) using the data of AL731576. Several possible transcription elements, such as the GC box (-12 and -187 of ADK gene), p53 response element (-252 and -585), and heat shock element (-559, -971, -1486, and -1797) were detected in up to approximately 2 kb upstream from the estimated transcription start point, but not in more 2 kb. Accordingly, we amplified approximately 2

kb including the 5' UTR (187 nts estimated by NM_001123 [31-OCT-2010]) by PCR using DNA prepared from ORL8 or OR6 cells, and each PCR product was inserted into pGL4.10-luc2 for the sequence analysis and reporter analysis of gene promoter activity. Sequence analysis confirmed that the sequences of the inserts were the same as the sequence data of the ADK gene (AL731576), except in the case of a single-nucleotide polymorphism (SNP) [rs10824095; C for ORL8 cells and T for OR6 cells] located 20 bases upstream from the initiation codon. Luciferase reporter assay using ORL8c cells revealed that the promoter activity of OR6 origin was almost equal to that of ORL8 origin (Supporting Fig. 4A), indicating that the detected SNP was not involved in the level of promoter activity.

We next evaluated the epigenetic effects on ADK expression level. The results revealed that the expression level of ADK mRNA in OR6 cells was not enhanced in the cells treated with 5azaC and/or 4-PBA for 48 hours (Supporting Fig. 4B). Moreover, the protein level of ADK was not increased in the OR6 cells treated with 5azaC for 6 days (Supporting Fig. 4C). Taken together, these results suggest that the low level of ADK mRNA in OR6 cells was not the result of genetic polymorphisms or epigenetic alternations in the ADK gene promoter region.

The Differential ADK Expression Between OR6 and ORL8 Cells Was Not Mediated by a microRNA Control Mechanism. To explain the above-described gap between the 4.5-fold difference in the mRNA level and the 16-fold difference in the protein level (Fig. 1C,E), we hypothesized that the 3' UTR of ADK mRNA was different in the length or nt sequences between OR6 and ORL8 cells, and that such differences affected the control mechanism by microRNA (miRNA). To test this hypothesis, we first performed 3' rapid amplification of cDNA ends (RACE) analysis on ADK mRNA using total RNA prepared from OR6 or ORL8 cells. Sequence analysis using more than 45 cDNA clones obtained from each cell line was carried out. 3' UTRs of four different lengths were detected in both OR6 and ORL8 cells, because four potential poly(A) additional signals were present in the downstream ADK open reading frame (ORF) (Supporting Fig. 5). The results revealed no qualitative difference of 3' UTR species between OR6 and ORL8 cells (Supporting Fig. 5).

Because the 3' UTR of ADK mRNA contained the seed sequences of miR-182, miR-203, miR-125a-3p, and miR-106b (Supporting Fig. 5), we assumed that

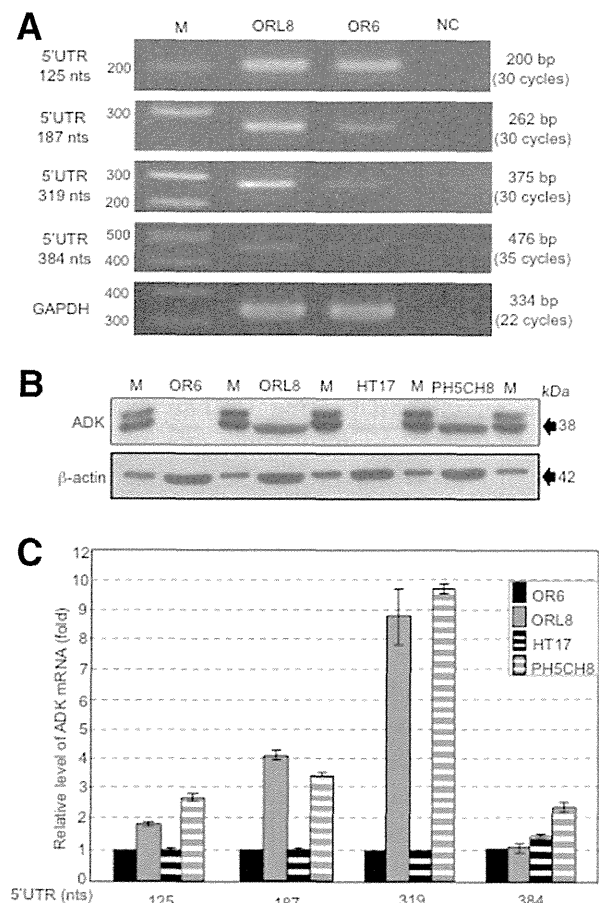


Fig. 3. Level of ADK mRNA possessing long 5' UTR was correlated with the expression level of ADK. (A) Total RNAs prepared from ORL8 and OR6 cells were subjected to RT-PCR using the primer sets (Supporting Table 1) for various lengths of 5' UTR of ADK mRNA. (B) Expression levels of ADK were compared by western blotting analysis. The two molecular markers of ADK shown in Fig. 1E were loaded on every two lanes. (C) Amounts of 5' UTR species of ADK mRNAs were compared by quantitative RT-PCR analysis using the primer sets described in (A). Experiments were performed in triplicate.

the difference in expression levels of these miRNAs causes the different protein levels of ADK. To examine this possibility, we performed a miRNA microarray analysis between OR6 and ORL8 cells. This analysis revealed very low expression levels (measured values of less than 7) of miR-182, miR203, and miR-125a-3p in both cell lines. Although only miR-106b was moderately expressed (measured value of approximately 300) in OR6 and ORL8 cells, the values obtained from both cell lines were almost the same. From these results, these miRNAs may not participate in the translational regulation of ADK mRNAs in OR6 and ORL8 cells.

The 5' UTR of ADK mRNA in ORL8 Cells Was Longer Than That in OR6 Cells. To explain the dramatic difference in ADK expression between ORL8

and OR6 cells, we next focused on the 5' UTR. To date, two different lengths of 5' UTR (384 nts in accession number NM_001123[25-MAR-2011] and 187 nts in accession numbers NM_001123[31-OCT-2010] and HSU_50196) have been deposited in GenBank. Because the 384 nts form has been considered to be a unique species in testis tissue, we performed 5' RACE analysis to determine the length of the 5' UTR of ADK mRNA in ORL8 or OR6 cells. Sequence analysis was carried out using more than 20 cDNA clones obtained from each cell line. Consequently, we obtained 319 and 125 nts as the major 5' UTR species in ORL8 and OR6 cells, respectively. We confirmed these results by RT-PCR analysis using four different primer sets for the 5' UTR (Fig. 3A). The amount of 384 nts species in ORL8 cells was estimated to be less than one thirtieth the amount of the 319-nts species (Fig. 3A). These results indicate that the length of 5' UTR in ORL8 cells is longer than that in OR6 cells.

From these results, we considered the possibility that the length of the 5' UTR is associated with the protein level of ADK. To test this possibility, we first compared the expression levels of ADK in various human hepatoma cell lines and human immortalized hepatocyte lines. Low expression level of ADK was observed in HT17 and Hep3B cells as well as OR6 cells, although the other cell lines, including ORL8, HuH-6, HepG2, HLE, and PH5CH8 cells, showed high expression level of ADK (Fig. 3B and Supporting Fig. 6). We next performed quantitative RT-PCR analysis on the 5' UTR using total RNAs from OR6, ORL8, HT17, and PH5CH8 cells. Consequently, we found that the 319 nts species of the 5' UTR was abundant in PH5CH8 cells, but not in HT17 cells (Fig. 3C), indicating good correlation between the amount of 319 nts species and the amount of ADK protein (Fig. 3B,C). These results suggest that the 319 nts species of 5' UTR is involved in the high protein level of ADK.

The Long-Form 5' UTR of ADK mRNA Possessed IRES Activity. From the results of 5' UTR analysis, we assumed that the 319 nts species of the 5' UTR possesses IRES activity because it is GC rich (72%) and highly structured (estimated $\Delta G = -110.7$ kcal/mol), and because it contains an upstream ORF for 70 amino acids. To test this assumption, we used a bicistronic dual luciferase reporter assay system for the detection of IRES activity (Fig. 4A). As a positive control, we constructed a pGL4-based reporter plasmid containing HCV IRES (377 nts; 341 nts in the 5' UTR plus the first 36 nts in the Core-encoding

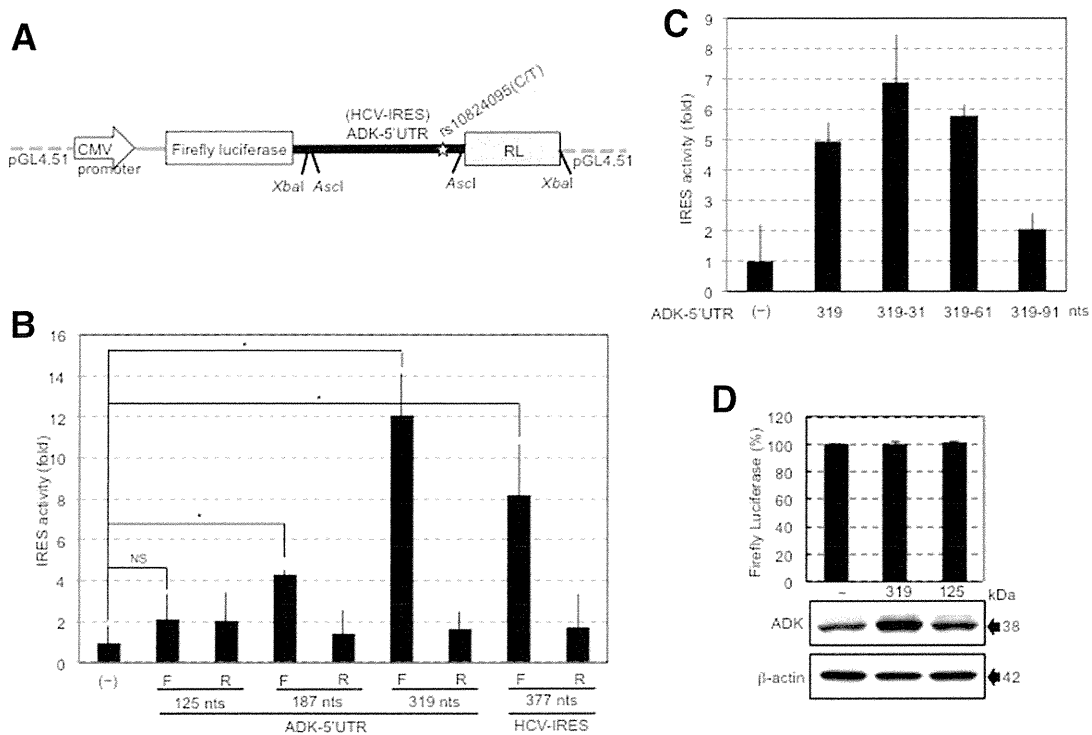


Fig. 4. Long-form 5' UTR of ADK mRNA possessed IRES activity. (A) Partial structure of the plasmid used as a dicistronic dual reporter assay system. (B) ORL8c cells were transfected with the plasmid as shown in (A). After 48 hours, a dual luciferase assay was performed. The ratio of the RL activity to firefly luciferase activity was calculated. The relative value calculated at each sample, when the ratio in the control vector-transfected cells (—) was assigned to be 1, is presented. F and R indicate the forward and reverse direction of insert in the reporter plasmid, respectively. (C) Deletion mutant analysis of the 5' UTR in IRES assay. IRES assay was performed using ORL8c cells transfected with the reporter plasmid containing the deleted forms of the 5' UTR, as described in (B). (D) ADK expression derived from the long-form 5' UTR transcript was more productive than that from the short-form 5' UTR transcript. OR6c cells were transfected with the plasmid, in which the XbaI fragment of the plasmid used for HCV IRES activity assay was replaced by the ADK ORF possessing the 5' UTR of 319 or 125 nts. After 48 hours, western blotting analysis was performed. Firefly luciferase activities were measured to check equal transfection efficiency. Experiments (B and C) were performed in triplicate. * $P < 0.05$; NS, not significant.

region). We next replaced the HCV IRES structure in this plasmid with several different lengths (forward or reverse direction) of the 5' UTR derived from ORL8 cells. ORL8c cells were transfected with these plasmids, and at 48 hours after transfection, dual luciferase assays were performed. Consequently, we found that the forward 319 nts, but not the forward 125 nts, of 5' UTR clearly showed IRES activity at the same level as HCV IRES (Fig. 4B). The 187 nts species also showed weak IRES activity (Fig. 4B). None of the 5' UTR species with reverse direction and none of the HCV IRES with reverse direction showed any IRES activities (Fig. 4B). Furthermore, similar results were obtained in the genome-length HCV RNA-replicating OL8 cells and their cured cells (OL8c) (Supporting Fig. 7A,B), suggesting that IRES activity does not depend on cell strains or HCV RNA replication. In addition, we did not observe any effects of an SNP (rs10824095), which was located 20 bases upstream from the initiation codon, on the IRES activities of

OR6 and ORL8 cell-derived 5' UTRs (319 nts) (Supporting Fig. 8).

To identify the entry site of the 40S ribosome in the IRES region, we prepared three deletion mutants (deleted upstream 30, 60, and 90 nts from the initiation codon) of the 5' UTR and measured their IRES activities in ORL8c cells. The results revealed that the deletion up to 60 nts from the initiation codon did not decrease IRES activity, but the 90 nts deletion abolished IRES activity (Fig. 4C). Similar results were also obtained in OL8 and OL8c cells (Supporting Fig. 7C,D). These results suggest that the entry site of the 40S ribosome is between 60 and 90 nts upstream from the initiation codon, and that the region from 319 to 61 nts upstream from the initiation codon is necessary for the IRES activity. It is noteworthy that this region forms a stable secondary structure (estimated $\Delta G = -108.4$ kcal/mol) (Supporting Fig. 7E). Furthermore, we demonstrated that ADK expression derived from the long-form 5' UTR transcript was

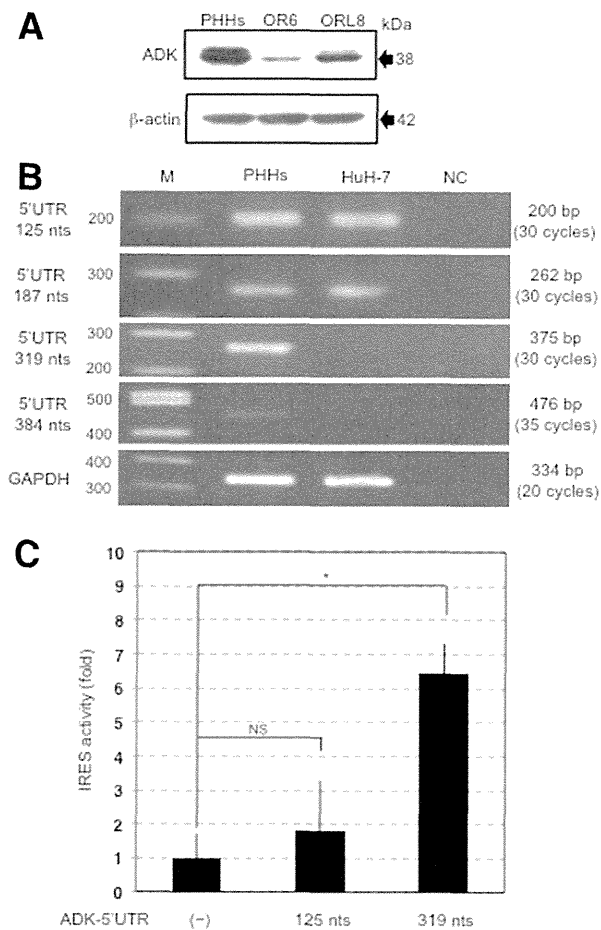


Fig. 5. Long-form 5' UTR of ADK mRNA functioned as an IRES in PHHs. (A) ADK expression level in PHHs was compared with those in OR6 and ORL8 cells by western blotting analysis. (B) Total RNAs prepared from PHHs and HuH-7 cells were subjected to RT-PCR analysis using the primer sets described in Fig. 3A. (C) PHHs were transfected with the plasmid shown in Fig. 4A. After 48 hours, a dual luciferase assay was performed as described in Fig. 4B. Experiments (B and C) were performed in triplicate. * $P < 0.05$; NS, not significant.

more productive than the expression from the short-form 5' UTR transcript in OR6c cells (Fig. 4D).

The Long-Form 5' UTR of ADK mRNA Functioned as an IRES in Primary Human Hepatocytes. To obtain a final conclusion, we examined whether the novel mechanism in ADK translation plays a role in PHHs. We first examined ADK expression level in PHHs, and the results revealed that ADK protein level was higher in PHHs than in ORL8 cells (Fig. 5A). We next performed RT-PCR analysis using the primer sets used in Fig. 3A to examine the amounts of 319 and 125 nts forms of the 5' UTR. The results showed that the 319 nts species was the major 5' UTR species in PHHs, but not in HuH-7 cells, which are the parent of OR6 cells (Fig. 5B), indicating a good correlation between the amount of 319 nts species and the amount of ADK protein in

PHHs. Finally, we demonstrated that the 319 nts form, but not the 125 nts form, of 5' UTR clearly showed IRES activity in PHHs (Fig. 5C).

Considering all these results together, we conclude that not only ORL8 cells, but also PHHs express the long-form 5' UTR of ADK mRNA possessing IRES activity and then produce high levels of ADK, which works as an RBV kinase.

Discussion

In this study, we identified, for the first time, a host factor ADK whose expression level could control the anti-HCV activity of RBV. Furthermore, we found that the expression level of ADK was associated with the amount of ADK mRNA possessing long 5' UTR exhibiting IRES activity. This finding suggests that the RBV sensitivity on HCV RNA replication is regulated by the IRES-dependent translation of ADK mRNA. If ADK expression levels or activity differ between patients with CHC, it may be a useful therapeutic target.

It has recently been reported that a functional SNP (rs1127354; major C and minor A) in inosine triphosphatase was the most significant SNP associated with RBV-induced anemia.¹⁸ In this context, we hypothesized that this SNP is associated with the expression level of ADK. To test this hypothesis, we examined the status of rs1127354 in ORL8 and PH5CH8 cells showing high expression levels of ADK and in OR6 and Hep3B cells showing low expression levels of ADK. The results revealed that all cell lines showed the major C of the SNP, suggesting that rs1127354 is not associated with the expression level of ADK.

The most striking highlight in this study is the IRES activity found in ADK mRNA. It has recently been reported that cellular IRES-mediated translation is activated by many physiological and pathological stress conditions in eukaryotic cells.¹⁹ To achieve efficient IRES-dependent translation, some triggers will be needed. However, HCV RNA replication was not such a trigger, in the present study, because a similar level of IRES activity was observed in both OL8c cured cells and genome-length HCV RNA-replicating OL8 cells (Supporting Fig. 7A-D). The addition of adenosine did not act as a trigger for IRES (Supporting Fig. 9). Another possible explanation for the high level of ADK in ORL8 cells would be the involvement of one or more miRNA(s) in stabilizing the IRES-containing ADK mRNA, as reported in HCV RNA.²⁰ To test this possibility, we performed comparative miRNA microarray analysis using ORL8, PH5CH8, OR6, and HT17 cells. The results revealed that nts 1-8 of miR-

424, whose expression levels in ORL8 and PH5CH8 cells were several times higher than those in OR6 and HT17 cells, showed base pairs in the nt 61-68 upstream initiation codon of ADK mRNA. It was noticed that this region in ADK mRNA overlaps the region (nt 60-90 upstream initiation codon of ADK mRNA) identified as the entry site of the 40S ribosome. However, a preliminary experiment showed that overexpression of miR-424 in ORL8 or OR6 cells did not enhance the translation of ADK (Supporting Fig. 10), suggesting that miR-424 is not associated with the high level of ADK in ORL8 cells. The possibility remains that other miRNA(s) participate in the up-regulation of ADK.

At this time, we have identified ADK as a host factor that controls the anti-HCV activity of RBV and clarified the molecular mechanism underlying regulation with ADK. Furthermore, we demonstrated that such a novel mechanism plays a role in PHHs. From our finding, we suggest that ADK expression is artfully regulated both at the transcription and translation stage. Although we identified ADK, which participates in nucleotide metabolism, as an enzyme functionally controlled by the specific expression of an IRES-containing mRNA, there may be other gene products controlled by a similar mechanism.

Acknowledgments: The authors thank Naoko Kawahara, Takashi Nakamura, and Keiko Takeshita for their technical assistance.

References

- Lindenbach BD, Rice CM. Unravelling hepatitis C virus replication from genome to function. *Nature* 2005;436:933-893.
- Ghany MG, Nelson DR, Strader DB, Thomas DL, Seeff LB. An update on treatment of genotype 1 chronic hepatitis C virus infection: 2011 practice guideline by the American Association for the Study of Liver Diseases. *HEPATOLOGY* 2011;54:1433-1444.
- Jacobson IM, McHutchison JG, Dusheiko G, Di Bisceglie AM, Reddy KR, Bzowej NH, et al. Telaprevir for previously untreated chronic hepatitis C virus infection. *N Engl J Med* 2011;364:2405-2416.
- Poordad F, McCone J, Jr., Bacon BR, Bruno S, Manns MP, Sulkowski MS, et al. Boceprevir for untreated chronic HCV genotype 1 infection. *N Engl J Med* 2011;364:1195-1206.
- Feld JJ, Hoofnagle JH. Mechanism of action of interferon and ribavirin in treatment of hepatitis C. *Nature* 2005;436:967-972.
- Paeshuyse J, Dallmeier K, Neyts J. Ribavirin for the treatment of chronic hepatitis C virus infection: a review of the proposed mechanisms of action. *Curr Opin Virol* 2011;1:590-598.
- Thomas E, Feld JJ, Li Q, Hu Z, Fried MW, Liang TJ. Ribavirin potentiates interferon action by augmenting interferon-stimulated gene induction in hepatitis C virus cell culture models. *HEPATOLOGY* 2011;53:32-41.
- Zhou S, Liu R, Baroudy BM, Malcolm BA, Reyes GR. The effect of ribavirin and IMPDH inhibitors on hepatitis C virus subgenomic replicon RNA. *Virology* 2003;310:333-342.
- Ikeda M, Abe K, Dansako H, Nakamura T, Naka K, Kato N. Efficient replication of a full-length hepatitis C virus genome, strain O, in cell culture, and development of a luciferase reporter system. *Biochem Biophys Res Commun* 2005;329:1350-1359.
- Mori K, Ikeda M, Ariumi Y, Dansako H, Wakita T, Kato N. Mechanism of action of ribavirin in a novel hepatitis C virus replication cell system. *Virus Res* 2011;157:61-70.
- Kato N, Mori K, Abe K, Dansako H, Kuroki M, Ariumi Y, et al. Efficient replication systems for hepatitis C virus using a new human hepatoma cell line. *Virus Res* 2009;146:41-50.
- Mori K, Ikeda M, Ariumi Y, Kato N. Gene expression profile of Li23, a new human hepatoma cell line that enables robust hepatitis C virus replication: comparison with HuH-7 and other hepatic cell lines. *Hepatology Res* 2010;40:1248-1253.
- Kato N, Sugiyama K, Namba K, Dansako H, Nakamura T, Takami M, et al. Establishment of a hepatitis C virus subgenomic replicon derived from human hepatocytes infected in vitro. *Biochem Biophys Res Commun* 2003;306:756-766.
- Dansako H, Naganuma A, Nakamura T, Ikeda F, Nozaki A, Kato N. Differential activation of interferon-inducible genes by hepatitis C virus core protein mediated by interferon stimulated response element. *Virus Res* 2003;97:17-30.
- Takatori S, Kanda H, Takenaka K, Wataya Y, Matsuda A, Fukushima M, et al. Antitumor mechanisms and metabolism of the novel antitumor nucleoside analogues, 1-(3-C-ethynyl-beta-D-ribo-pentofuranosyl)-cytosine and 1-(3-C-ethynyl-beta-D-ribo-pentofuranosyl)uracil. *Cancer Chemother Pharmacol* 1999;44:97-104.
- Streeter DG, Witkowski JT, Khare GP, Sidwell RW, Bauer RJ, Robins RK, Simon LN. Mechanism of action of 1-beta-D-ribofuranosyl-1,2,4-triazole-3-carboxamide (Virazole), a new broad-spectrum antiviral agent. *Proc Natl Acad Sci U S A* 1973;70:1174-1178.
- Cui XA, Singh B, Park J, Gupta RS. Subcellular localization of adenosine kinase in mammalian cells: the long isoform of AdK is localized in the nucleus. *Biochem Biophys Res Commun* 2009;388:46-50.
- Fellay J, Thompson AJ, Ge D, Gumbs CE, Urban TJ, Shianna KV, et al. ITPA gene variants protect against anaemia in patients treated for chronic hepatitis C. *Nature* 2010;464:405-408.
- Komar AA, Hatzoglou M. Cellular IRES-mediated translation: the war of ITAFs in pathophysiological states. *Cell Cycle* 2011;10:229-240.
- Shimakami T, Yamane D, Jangra RK, Kempf BJ, Spaniel C, Barton DJ, Lemon SM. Stabilization of hepatitis C virus RNA by an Ago2-miR-122 complex. *Proc Natl Acad Sci U S A* 2012;109:941-946.

Class A Scavenger Receptor 1 (MSR1) Restricts Hepatitis C Virus Replication by Mediating Toll-like Receptor 3 Recognition of Viral RNAs Produced in Neighboring Cells

Hiromichi Dansako^{1,2}, Daisuke Yamane¹, Christoph Welsch^{1✉}, David R. McGivern¹, Fengyu Hu¹, Nobuyuki Kato², Stanley M. Lemon^{1*}

1 Division of Infectious Diseases, Department of Medicine, and the Lineberger Comprehensive Cancer Center, The University of North Carolina at Chapel Hill, Chapel Hill, North Carolina, United States of America, **2** Department of Tumor Virology, Okayama University Graduate School of Medicine, Dentistry, and Pharmaceutical Science, Okayama, Japan

Abstract

Persistent infections with hepatitis C virus (HCV) may result in life-threatening liver disease, including cirrhosis and cancer, and impose an important burden on human health. Understanding how the virus is capable of achieving persistence in the majority of those infected is thus an important goal. Although HCV has evolved multiple mechanisms to disrupt and block cellular signaling pathways involved in the induction of interferon (IFN) responses, IFN-stimulated gene (ISG) expression is typically prominent in the HCV-infected liver. Here, we show that Toll-like receptor 3 (TLR3) expressed within uninfected hepatocytes is capable of sensing infection in adjacent cells, initiating a local antiviral response that partially restricts HCV replication. We demonstrate that this is dependent upon the expression of class A scavenger receptor type 1 (MSR1). MSR1 binds extracellular dsRNA, mediating its endocytosis and transport toward the endosome where it is engaged by TLR3, thereby triggering IFN responses in both infected and uninfected cells. RNAi-mediated knockdown of MSR1 expression blocks TLR3 sensing of HCV in infected hepatocyte cultures, leading to increased cellular permissiveness to virus infection. Exogenous expression of Myc-MSR1 restores TLR3 signaling in MSR1-depleted cells with subsequent induction of an antiviral state. A series of conserved basic residues within the carboxy-terminus of the collagen superfamily domain of MSR1 are required for binding and transport of dsRNA, and likely facilitate acidification-dependent release of dsRNA at the site of TLR3 expression in the endosome. Our findings reveal MSR1 to be a critical component of a TLR3-mediated pattern recognition receptor response that exerts an antiviral state in both infected and uninfected hepatocytes, thereby limiting the impact of HCV proteins that disrupt IFN signaling in infected cells and restricting the spread of HCV within the liver.

Citation: Dansako H, Yamane D, Welsch C, McGivern DR, Hu F, et al. (2013) Class A Scavenger Receptor 1 (MSR1) Restricts Hepatitis C Virus Replication by Mediating Toll-like Receptor 3 Recognition of Viral RNAs Produced in Neighboring Cells. *PLoS Pathog* 9(5): e1003345. doi:10.1371/journal.ppat.1003345

Editor: Karen L. Mossman, McMaster University, Canada

Received: September 5, 2012; **Accepted:** March 23, 2013; **Published:** May 23, 2013

Copyright: © 2013 Dansako et al. This is an open-access article distributed under the terms of the Creative Commons Attribution License, which permits unrestricted use, distribution, and reproduction in any medium, provided the original author and source are credited.

Funding: This work was supported in part by grants from the National Institutes of Health (RO1-AI095690) and the University Cancer Research Fund. The funders had no role in study design, data collection and analysis, decision to publish, or preparation of the manuscript.

Competing Interests: The authors have declared that no competing interests exist.

* E-mail: smlemon@med.unc.edu

✉ Current address: Department of Internal Medicine I, J.W. Goethe University Hospital, Frankfurt/Main, Germany.

Introduction

Hepatitis C virus (HCV) is an hepatotropic, positive-strand RNA virus classified within the *Flaviviridae* family [1]. It is an important human pathogen since most individuals fail to eliminate the virus when first infected. This results in persistent infection and a chronic inflammatory state within the liver that leads over time to clinically significant complications including progressive liver fibrosis, cirrhosis, and hepatocellular carcinoma. The mechanisms underlying these events are only partially understood. The single-stranded RNA (ssRNA) HCV genome encodes a large polyprotein precursor of approximately 3000 amino acid residues. This is cleaved co- and post-translationally into at least 10 mature proteins, at least 3 of which contribute to the virus structure (core, and two envelope proteins, E1 and E2), with the remaining 7 proteins generally considered to be nonstructural in nature (p7, NS2, NS3, NS4A, NS4B, NS5A, and NS5B). NS5B is an RNA-dependent RNA polymerase and the catalytic core of a large

macromolecular, membrane-bound replicase complex that directs replication of the viral RNA, producing double-stranded RNA (dsRNA) replication intermediates as well as new viral genomes. These viral RNAs are recognized as pathogen-associated molecular patterns (PAMPs) by innate immune sensors in host cells, but exactly which sequences and how these RNAs are sensed remains only partly elucidated [2].

In general, dsRNAs produced by viruses are recognized by several classes of cellular pattern recognition receptors, including retinoic acid-inducible gene I (RIG-I)-like helicases that are expressed within the cytoplasm, or Toll-like receptors (TLRs), such as TLR-3 that is expressed within and signals from a late endosomal compartment in several different cell types, including hepatocytes [3,4,5,6]. The engagement of these receptors by viral RNAs results in the induction of interferon (IFN)- β synthesis through separate downstream signaling pathways that utilize unique adaptor molecules but result in the common activation of the transcription factors NF- κ B and IFN regulatory factor 3 (IRF-

Author Summary

Persistent hepatitis C virus (HCV) infection is an important cause of fatal cirrhosis and liver cancer in humans. While viral disruption of interferon (IFN) signaling pathways may contribute to the persistence of HCV, IFN-stimulated gene (ISG) expression is often prominent within the infected liver. We show here that this is due, at least in part, to Toll-like receptor 3 sensing of HCV mediated by class A scavenger receptor type 1 (MSR1)-dependent endocytosis and transport of extracellular viral double-stranded RNA (dsRNA) allowing it to be engaged by TLR3 in the late endosome. TLR3 expressed within uninfected cells is capable of sensing HCV infection in neighboring infected cells in a process that is dependent upon the dsRNA-scavenging activity of MSR1, resulting in the induction of a localized functional antiviral response. This contributes to the ISG expression that typifies the chronically-infected liver, as it occurs within cells that do not express HCV proteins that disrupt IFN signaling. TLR3 signaling thus limits the spread of virus within the liver, potentially explaining why only a small fraction of hepatocytes are infected with HCV *in vivo*.

3) [reviewed in 7]. This leads in turn to the expression of numerous IFN-inducible genes, including IFN-stimulated gene (ISG)15, ISG56, and others, through both autocrine and paracrine signaling involving the Janus kinase/signal transducer and activator of transcription (JAK/STAT) pathway. RIG-I, and the related cytosolic helicase, myeloid differentiation-associated gene 5 (MDA5) and TLR3 differ substantially in their ligand specificities. RIG-I recognizes short dsRNA molecules and ssRNA with a 5'-triphosphate, while MDA5 recognizes lengthy dsRNA [5,8]. In addition, the roles played by RIG-I (which is generally constitutively expressed) and MDA5 (IFN-inducible) in recognition of RNA viruses appear to vary by virus type. RIG-I is primarily responsible for innate immune recognition of paramyxoviruses, influenza virus and Japanese encephalitis virus, while MDA5 is thought to be critical for the recognition of encephalomyocarditis virus and possibly other picornaviruses [5]. TLR3 recognizes dsRNA molecules greater than 40–50 bp in length and also mediates the induction of antiviral responses in cells infected with a wide variety of RNA viruses, including West Nile virus, rhinovirus, respiratory syncytial virus, vesicular stomatitis virus, lymphocytic choriomeningitis virus and influenza virus [9,10]. However, unlike the cytosolic RIG-I-like helicases, TLR3 initiates signaling from within the endosome in a process that is dependent upon acidification of the endosome [11,12].

In HCV-infected cells, the 5'-triphosphate of genomic RNA is recognized by RIG-I, as is a poly-U/UC segment near the 3' end of the genome that serves as a PAMP [13,14]. This results in the induction of an IFN response shortly after infection of cells [14]. However, RIG-I-initiated signaling is subsequently blocked since NS3/4A, the major HCV protease, proteolytically cleaves the essential RIG-I adaptor protein, mitochondrial antiviral signaling protein (MAVS) [14,15,16]. The only continuous cell lines that support robust HCV replication are derived from Huh-7 human hepatoma cells, which like many transformed hepatocytes are TLR3 null [17]. However, HCV infection similarly induces an early antiviral response in RIG-I-defective Huh-7.5 cells in which TLR3 expression has been reconstituted [4]. As with RIG-I signaling, TLR3 signaling is also blocked as viral proteins accumulate and NS3/4A mediates cleavage of an essential adaptor protein, in this case Toll-like receptor adaptor molecule 1

(TICAM-1, a.k.a. TRIF) [4,18]. How TLR3 is able to sense HCV infection is uncertain, since double-stranded HCV RNA is detected primarily adjacent to ER membranes in association with the nonstructural protein, NS5A, or juxtaposed to cytoplasmic lipid droplets [19], while TLR3, as described above, senses dsRNA and initiates signaling only from within late endosomes [11,12].

One possibility is that dsRNA replication intermediates are released into the extracellular milieu by HCV-infected cells and, like poly(I:C) added to the medium of cultured cells, subsequently sensed by TLR3. Since TLR3 is unable to bind extracellular dsRNA on the cell surface [12], this would require a receptor molecule to direct the endocytosis and trafficking of dsRNA to the late endosome. Scavenger receptors of several different classes, including C-type lectin domain-containing receptors such as the oxidized low density lipoprotein (LDL) receptor (ORL-1), or class A scavenger receptors such as macrophage scavenger receptor 1 (MSR1), have been suggested to fulfill this function, transporting dsRNA from the surface of cells to the endosome where it is sensed by TLR3 [20,21,22]. The epidermal growth factor receptor (EGFR) also plays an essential role in TLR3 signaling, but this appears to occur at a later step, following the engagement of TLR3 by dsRNA within the endosome [23].

Here, we show that MSR1 is essential for TLR3 sensing of HCV infection in cells derived from human hepatocytes, and that it mediates the establishment of a localized antiviral response in neighboring, uninfected cells that restricts the replication of virus in cell culture. Since uninfected hepatocytes are not subject to the myriad mechanisms that virally-encoded HCV proteins have evolved to disrupt the induction of IFN responses [2], these observations reveal a mechanism that may explain both the significant levels of ISG expression that typify the HCV-infected liver [24], as well as the fact that only a small minority of hepatocytes are infected by HCV in human liver [25].

Results

Replication intermediates trigger TLR3 signaling in HCV-infected cells

While TLR3 is expressed and functional in primary cultures of human hepatocytes, Huh-7 cells and their derivatives have a TLR3-null phenotype [4,17]. Thus, to establish an HCV-permissive cell line in which we could study viral interactions with the TLR3 signaling pathway, we reconstituted TLR3 expression in Huh-7.5 cells, which are also RIG-I-deficient [4,26]. Using this, and related cell lines, we demonstrated previously that HCV infection is sensed by TLR3, resulting in an early antiviral response [4]. However, HCV ultimately restricts TLR3 signaling as the NS3/4A protease mediates cleavage of TICAM-1 as viral proteins accumulate in abundance [4,18]. To further confirm that TLR3 induces a functional antiviral response against HCV, we compared the number of colonies of viable cells originating from TLR3-competent Huh7.5-TLR3 cells transfected with a dicistronic, genome-length HCV replicon that expresses neomycin phosphotransferase [pTat2ANeo/H77S, 27] versus similarly transfected TLR3-null Huh-7.5 cells reconstituted with non-functional TLR3 mutants. As expected, the number of G418-resistant colonies arising from Huh7.5-TLR3 cells was significantly lower than from several related, TLR3-null Huh-7.5 cell lines: Huh-7.5-Vect (empty vector), $-\Delta$ TIR (TLR3 lacking the TIR domain required for downstream signaling), and $-H539E$ and $-N541A$ (point mutations in the ectodomain of TLR3 that restrict its ability to bind dsRNA) (Supplementary Fig. S1). Consistent with these results, quantitative real-time PCR demonstrated

significant increases in the abundance of IFN- β and ISG56 mRNAs in Huh7.5-TLR3 cells following infection with a laboratory strain of HCV (HJ3-5 virus) (Fig. 1A, left and center panels). Similar increases were not observed in Huh-7.5 cells expressing the signaling-incompetent TLR3 mutants H539E or N541A. Importantly, prior UV inactivation of the virus (UV-HCV) almost completely eliminated the increase in ISG56 mRNA (Fig. 1A, right panel). On the basis of these and our previously published results [4], we conclude that TLR3 senses HCV infection and induces the expression of a functional antiviral state in Huh7.5-TLR3 cells, and that this requires active replication of the virus. This is consistent with a recent report indicating that

TLR3-mediated induction of proinflammatory cytokines by HCV also requires active replication of virus [28].

To better understand these results, we examined the ability of in vitro synthesized HCV RNAs to stimulate TLR3 signaling. Since replication of the virus is required to initiate signaling, we reasoned that TLR3 signaling follows its engagement by dsRNA molecules produced by transcription of negative-strand RNA intermediates, rather than multiple structured RNA elements that are known to exist within the 5' and 3' untranslated regions as well as in the core and NS5B protein-coding regions of the positive-strand genome [29]. To test this, we synthesized full-length positive- and negative-strand viral RNAs by in vitro transcription using as template an

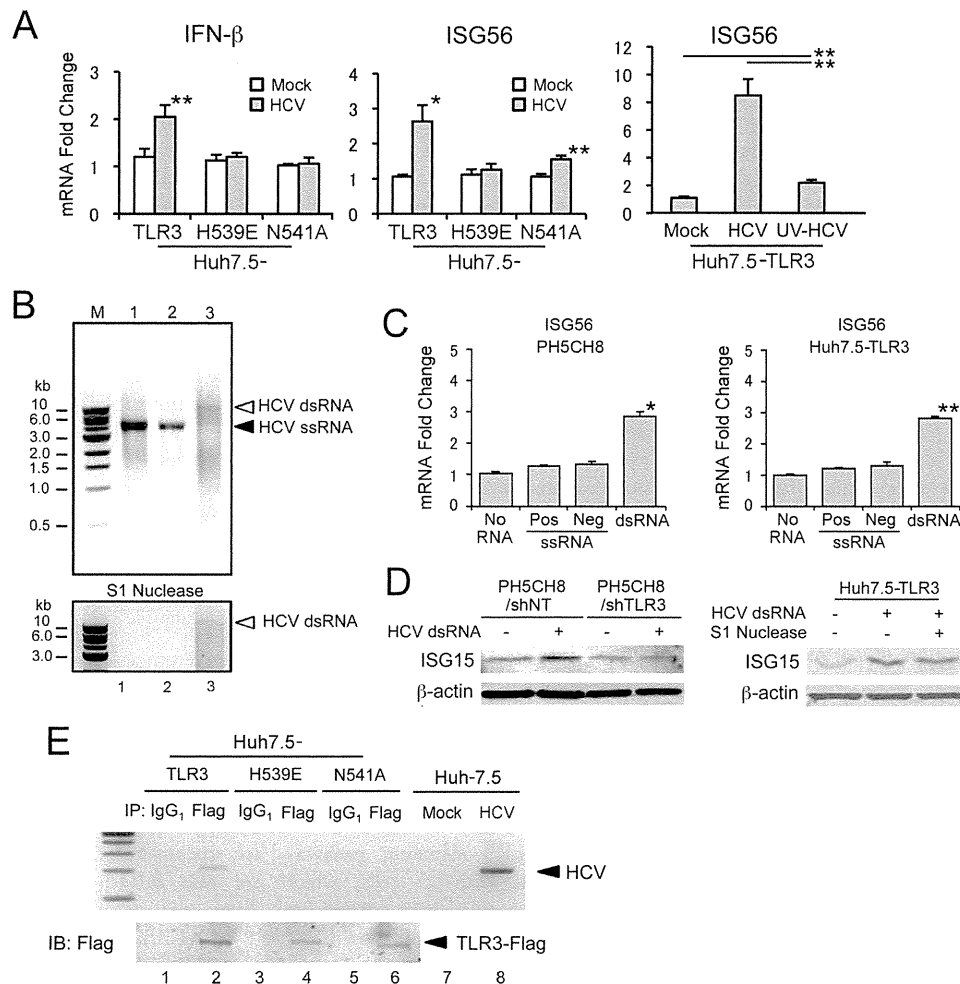


Figure 1. TLR3 senses double-stranded RNA products of HCV replication in human hepatocytes. (A) Quantitative RT-PCR analysis of (left) IFN- β and (center and right) ISG56 mRNA in Huh7.5-TLR3 cells infected with HCV. Cells were infected with HCV (HJ3-5) or UV-inactivated HCV at an m.o.i. of 1 for 72 hrs, prior to extraction of RNA and measurement of IFN- β and ISG56 mRNA. Statistical comparisons were made between mock- and HCV-infected cultures (left and center panels), or between samples indicated by bars (right panel): * $p \leq 0.02$, ** $p \leq 0.001$. (B) Agarose gel electrophoresis of in vitro transcribed HCV RNAs (top panel) before or (bottom panel) after S1 nuclease treatment. M: DNA standards ladder; lane 1, positive-strand HCV RNA; lane 2, negative-strand HCV RNA; lane 3, annealed double-stranded HCV RNA. (C) Quantitative RT-PCR analysis of ISG56 mRNA in (left) PH5CH8 and (right) Huh7.5-TLR3 cells treated with 50 μ g/ml of ssRNA or dsRNA for 6 hrs prior to extraction of RNA. Statistical comparisons were made with cultures not treated with RNA: * $p \leq 0.02$, ** $p \leq 0.001$. (D) (left panel) Immunoblot analysis of ISG15 expression induced by synthetic HCV dsRNA in PH5CH8 cells previously transduced with lentivirus vectors expressing non-targeting (NT) or TLR3-specific shRNAs. β -actin was included as a loading control. (right panel) Similar immunoblots of Huh7.5-TLR3 cells treated with HCV dsRNA, either with or without prior S1 nuclease digestion. In both panels, cell lysates were prepared for immunoblotting 24 hrs after addition of dsRNA. (E) HCV RNA co-immunoprecipitates with Flag-TLR3 from lysates of HCV-infected Huh7.5-TLR3 cells. (top panel) Agarose gel electrophoresis showing detection of HCV-specific RNA by RT-PCR in anti-Flag (lanes 2, 4 and 6), or isotype control (mouse IgG₁, lanes 1, 3 and 5), immunoprecipitates prepared from lysates of Huh7.5-TLR3 cells (lanes 1 and 2), Huh7.5-H539E cells (lanes 3 and 4), or Huh7.5-H539E cells (lanes 5 and 6), infected with HJ3-5 virus (m.o.i. = 1) for 72 hrs. RNA extracted from mock or HCV-infected Huh7.5 cells was assayed in parallel in the RT-PCR reaction as negative and positive controls, respectively (lanes 7 and 8). (bottom panel) Anti-Flag immunoblots of the respective immunoprecipitates.

infectious molecular clone of the genotype 2a JFH1 strain (Fig. 1B, upper panel, lanes 1 and 2), and annealed these to produce HCV dsRNA (Fig. 1B, lane 3). As anticipated, the dsRNA products produced by annealing the two ssRNAs were highly heterogeneous, resulting in a smear when separated by agarose gel electrophoresis. However, a small amount of what appeared to be full-length dsRNA was generated (Fig. 1B, arrow). While the positive- and negative-sense ssRNAs were degraded by S1 nuclease, this dsRNA was S1 nuclease-resistant, confirming that the complementary *in vitro* synthesized HCV RNAs anneal to produce dsRNA (Fig. 1B, lower panel). Importantly, only the nuclease-resistant dsRNA induced transcription of ISG56 mRNA when added to the medium of PH5CH8 cells, a T-antigen transformed, human hepatocyte line that naturally expresses TLR3, or Huh7.5-TLR3 cells [30] (Fig. 1C, left and right panels). HCV dsRNA also induced ISG15 protein expression in PH5CH8 and Huh7.5-TLR3 cells (Fig. 1D). Prior transfection of PH5CH8 cells with shRNA targeting TLR3 eliminated the induction of ISG15 protein expression by HCV dsRNA (Fig. 1D, left panel), confirming that ISG15 induction was mediated through TLR3. Prior digestion of the dsRNA with S1 nuclease did not alter the pattern of ISG15 induction (Fig. 1D right panel). Collectively, these data indicate that S1-resistant, double-stranded synthetic HCV RNA is capable of triggering an antiviral response through TLR3, while highly structured RNA elements of the single-stranded genome are not sensed by TLR3. In part, this may be due to the length of the synthetic dsRNAs, which mimic very lengthy dsRNA intermediates produced during replication of the 9.7 kb HCV genome (Fig. 1B) and are much longer than the stable helices present in the ssRNA. While the minimum length of dsRNA required for recognition by the TLR3 ectodomain is on the order of 40 to 50 base pairs [31], we have observed that TLR3 is substantially more responsive to high-molecular weight (1.5–8.0 kb) versus low molecular weight poly(I:C) (0.2–1.0 kb) (Supplementary Fig. S2).

Consistent with the induction of a TLR3-mediated antiviral response by HCV, we detected formation of a TLR3-HCV RNA complex in Huh7.5-TLR3 cells infected with HJ3-5 virus. This was accomplished by immunoprecipitating TLR3 from lysates of infected Huh7.5-TLR3 cells with an anti-Flag antibody, and subjecting RNA extracted from the precipitates to RT-PCR specific for HCV RNA. Viral RNA was readily detected in anti-Flag precipitates prepared from lysates of infected Huh7.5-TLR3 cells (Fig. 1E, lane 2). While somewhat less Flag product was evident in immunoblots of precipitates from cells expressing TLR3-H539E or TLR3-N541A, TLR3 mutants deficient in binding dsRNA [4], HCV RNA was not detected in these precipitates (Fig. 1E, lanes 4 and 6). Taken together, these results indicate that dsRNA produced in membrane-bound replicase complexes during HCV replication is transported to the late endosome where it is engaged by TLR3. Subsequent experiments focused on the mechanism by which dsRNA traffics to the endosome.

Macrophage scavenger receptor 1 (MSR1) is required for TLR3 engagement by HCV RNA

Recent studies suggest that class A scavenger receptors, including “macrophage” scavenger receptor 1 (MSR1, class A scavenger receptor type 1, transcript variant 1), are expressed in a variety of cell types and serve as the dominant receptors mediating endocytosis of dsRNA in fibroblasts [20,22]. Class A scavenger receptors recognize a broad range of ligands including acetylated LDL, and lipopolysaccharide (LPS) produced by Gram-positive bacteria, and have been shown to mediate endocytosis of both ssRNA and dsRNA [22,32]. We thus hypothesized that dsRNA

could be released into the extracellular milieu by hepatocytes infected with HCV, where it could be bound by scavenger receptors expressed on the cell surface and subsequently transported to the endosome for recognition by TLR3. To confirm that MSR1, and possibly other members of the class A scavenger receptor family, are expressed by human hepatocytes, we utilized RT-PCR to ascertain the presence of mRNA transcripts for these proteins in PH5CH8 cells. Transcripts encoding MSR1 (SCARA1, transcript variant 1, referred to generally as “MSR1”), scavenger receptor class A member 3 (SCARA3, transcript variants 1 and 2), SCARA4 (a.k.a. collectin sub-family member 12, COLEC12), and SCARA5 (a putative class A scavenger receptor) transcripts were readily detected (Fig. 2A). Transcripts for MSR1 transcript variant 2 (referred to as “SR-AII”), and MARCO (a.k.a. SCARA2) were not detected, or were present only in very low abundance. MSR1 and SCARA3,

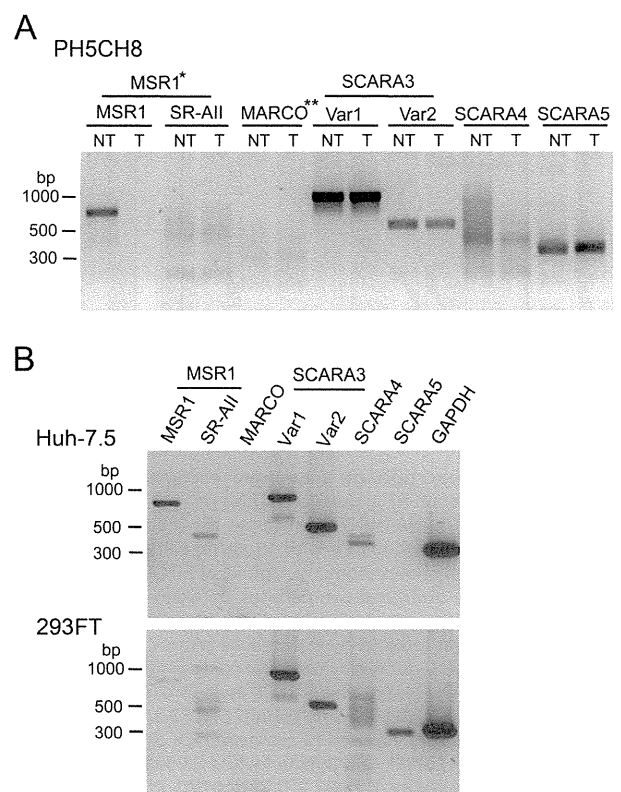


Figure 2. Scavenger receptor class A family transcript profiling of human hepatocyte-derived cell lines. (A) RT-PCR detection of class A scavenger receptor mRNAs in total cellular RNAs extracted from PH5CH8 cells transduced to express (“NT”) a non-targeting shRNA (PH5CH8/shNT cells), or (“T”) MSR1-specific shRNA (PH5CH8/shMSR1 cells). The parental PH5CH8 cells are T-antigen transformed normal adult human hepatocytes. Primers specific for MSR1 (SCARA1) transcript variant 1 (MSR1, SR-AI, or CD204) and transcript variant 2 (SR-AII), MARCO (SCARA2), SCARA3 (transcript variants 1 and 2), SCARA4, and SCARA5 (a putative scavenger receptor class A family member) were identical to those used by DeWitte-Orr et al. [22]. PCR was carried through 35 cycles prior to separation of products on an agarose gel. (B) Similar class A scavenger receptor transcript profiling of Huh-7.5 cells derived from a human hepatocellular carcinoma, and 293FT cells (Invitrogen). *MSR1 has two transcript variants: variant 1 is commonly referred to as “MSR1”, as we refer to it here, but is otherwise known as SCARA1 or SR-AI. Transcript variant 2 is referred to as SR-AII. See text for additional details. **MARCO, macrophage receptor with collagenous structure, is otherwise known as SCARA2. doi:10.1371/journal.ppat.1003345.g002

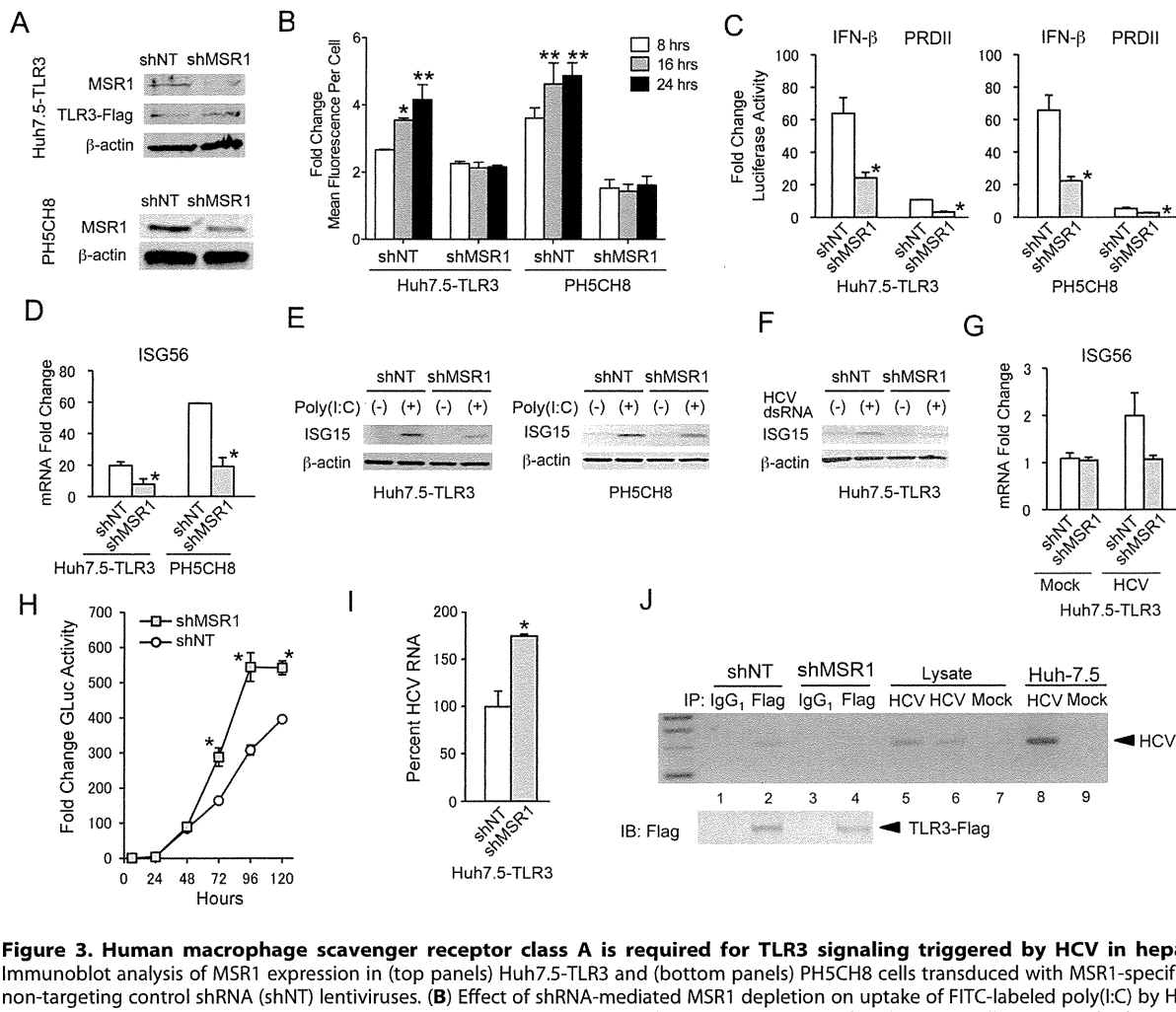


Figure 3. Human macrophage scavenger receptor class A is required for TLR3 signaling triggered by HCV in hepatocytes. (A) Immunoblot analysis of MSR1 expression in (top panels) Huh7.5-TLR3 and (bottom panels) PH5CH8 cells transduced with MSR1-specific (shMSR1) or non-targeting control shRNA (shNT) lentiviruses. (B) Effect of shRNA-mediated MSR1 depletion on uptake of FITC-labeled poly(I:C) by Huh7.5-TLR3 or PH5CH8 cells. Cells were incubated with 10 μ g/ml FITC-labeled poly(I:C) for 8, 16 or 24 hrs before harvest. Cells were washed extensively before fixation and analyzed by flow cytometry. Uptake of FITC-labeled poly(I:C) is expressed as fold-change in mean fluorescence intensity (MFI) compared to mock-treated cells. Statistical comparisons between the MFI at 8 hrs vs. the time indicated were made by two-way ANOVA with Bonferroni correction for multiple comparisons: * $p \leq 0.02$, ** $p \leq 0.001$. (C) Effect of shRNA-mediated MSR1 depletion on TLR3 signaling. IFN- β and PRD-II promoter activation was induced by extracellular poly(I:C) in MSR1-depleted (left) Huh7.5-TLR3 and (right) PH5CH8 cells exposed to 50 μ g/ml of high molecular weight poly(I:C) for 6 hrs. Statistical comparisons in this and other panels in this figure were between the shNT and shMSR1-treated cells: * $p \leq 0.02$, ** $p \leq 0.001$. (D) Quantitative RT-PCR analysis of ISG56 mRNA in MSR1-depleted cells treated with poly(I:C) as in panel C. (E) Immunoblots of ISG15 expression in MSR1-depleted (left) Huh7.5-TLR3 and (right) PH5CH8 cells treated with poly(I:C) for 24 hrs. (F) Immunoblot of ISG15 in MSR1-depleted Huh7.5-TLR3 cells exposed to synthetic HCV dsRNA 50 μ g/ml for 24 hrs. (G) Quantitative RT-PCR analysis of ISG56 mRNA in Huh7.5-TLR3/shMSR1 or Huh7.5-TLR3/shNT cells infected with HJ3-5 virus at an m.o.i. of 1 for 72 hrs. (H) Viral replication assessed by the fold-change in secreted *Gaussia* luciferase activity in cultures of Huh7.5-TLR3/shMSR1 vs. Huh7.5-TLR3/shNT cells following infection with HJ3-5/Gluc2A virus. The level of *Gaussia* luciferase activity at each time point was calculated relative to that at 6 hrs after infection, which was set at 1. Data are the mean \pm s.d. from three independent experiments. The difference in GLuc expression by Huh7.5-TLR3/shMSR1 vs. Huh7.5-TLR3/shNT cells was significant by two-way ANOVA ($p = 0.006$). Bonferroni post-tests were used to estimate the significance of differences at individual time points: * $p \leq 0.02$. (I) Quantitative RT-PCR analysis of HCV RNA in Huh7.5-TLR3/shMSR1 vs. Huh7.5-TLR3/shNT cells 72 hrs after infection with HCV. RNA abundance in the Huh7.5-TLR3/shMSR1 was calculated relative to that in Huh7.5-TLR3/shNT, which was set at 100%. (J) Co-immunoprecipitation of HCV RNA with Flag-TLR3 in lysates of Huh7.5-TLR3/shMSR1 (lanes 3, 4, and 6) and Huh7.5-TLR3/shNT cells (lanes 1, 2 and 5) infected with HJ3-5 virus 72 hrs previously. Immunoprecipitation was with anti-Flag. See legend to Fig. 1E for additional details.

variants 1 and 2, expression were also confirmed in Huh-7.5 cells (Fig. 2B, top panel). However, in contrast to PH5CH8 cells, SR-AII transcripts were also evident in Huh-7.5 cells, while SCARA5 transcripts were absent.

Consistent with these results, immunoblots demonstrated expression of MSR1 in both Huh7.5-TLR3 and PH5CH8 cells (Fig. 3A). To determine whether it plays a role in TLR3 signaling in these hepatocyte-derived cell lines, we depleted MSR1 by transducing Huh7.5-TLR3 cells (Huh7.5-TLR3/shMSR1 cells) and PH5CH8 cells (PH5CH8/shMSR1 cells) with lentiviruses

expressing MSR1-specific shRNA. Immunoblots demonstrated modest depletion of MSR1 in both Huh7.5-TLR3/shMSR1 cells (63% depletion estimated by quantitation of the Odyssey infrared fluorescence signal against β -actin control) and PH5CH8/shMSR1 cells (55% depletion). RT-PCR confirmed MSR1 knockdown in the PH5CH8 cells, and demonstrated that it was specific and without effect on SCARA3, SCARA4, or SCARA5 transcripts (Fig. 2A). Additional studies showed that MSR1 knockdown had no reciprocal effect on the abundance of SR-AII transcripts (data not shown). Although the MSR1 knockdown

was relatively inefficient in both cell types, flow cytometry indicated that time-dependent uptake of FITC-labeled high molecular weight (HMW) poly(I:C), a surrogate for HCV dsRNA, was functionally eliminated in MSR1-depleted cells compared to control cells (Fig. 3B). The high degree of inhibition of poly(I:C) uptake was surprising, given the rather modest degree of MSR1 depletion evident in either cell type (Fig. 3A). It suggests that a threshold level of expression is required for efficient dsRNA uptake, possibly because class A scavenger receptors function as multimeric complexes. IFN- β and NF- κ B-responsive PRDII promoter activities were also decreased in MSR1-depleted cells compared to control cells when stimulated by the addition of poly(I:C) to the medium (Fig. 3C), as was poly(I:C) induction of ISG56 (Fig. 3D) and ISG15 (Fig. 3E) expression. These results indicate that MSR1 is required for poly(I:C) uptake and optimal induction of TLR3-mediated signaling by poly(I:C) in human hepatocytes.

Next, we examined whether MSR1 is required for the recognition of HCV-specific dsRNA through TLR3. As with poly(I:C), MSR1 depletion eliminated the induction of ISG15 or ISG56 by synthetic HCV dsRNA added to the medium bathing Huh7.5-TLR3 cells (Fig. 3F and G). We also demonstrated that MSR1 functions in the induction of TLR3-mediated antiviral responses to HCV infection by monitoring viral replication in Huh7.5-TLR3/shNT cells and Huh7.5-TLR3/shMSR1 cells following infection with HJ3-5/GLuc2A virus [33] that expresses the secreted reporter protein, *Gaussia princeps* luciferase (GLuc). Replication was assessed by measuring secreted GLuc activity and by qRT-PCR analysis of intracellular HCV RNA abundance. Both GLuc activity (Fig. 3H) and HCV RNA abundance (Fig. 3I) were significantly increased in MSR1-depleted TLR3-expressing cells compared to control cells transduced with shNT, suggesting at least partial release from a TLR3-mediated antiviral response in these cells. Consistent with a role for MSR1 in transporting HCV RNA to the endosome where it can engage TLR3, HCV RNA was no longer detected in immunoprecipitates of TLR3 prepared from lysates of infected, MSR1-depleted cells (Fig. 3J, lane 4 vs. lane 2).

To exclude the unlikely possibility that these results might in some way reflect an off-target effect of shMSR1, we reconstituted MSR1 expression in Huh7.5-TLR3/shMSR1 cells by ectopic expression of Myc-tagged MSR1 using an expression vector lacking the 5' untranslated RNA (UTR) segment of the endogenous MSR1 mRNA targeted by shMSR1 (Fig. 4A). As we anticipated, poly(I:C) stimulation of IFN- β promoter activity was substantially restored by stable expression of Myc-MSR1 in Huh7.5-TLR3/shMSR1 cells ("Myc-MSR1 cells") (Fig. 4B). In addition, HCV RNA replication levels were reduced in HCV-infected Myc-MSR1 cells compared to Huh7.5-TLR3/shMSR1 cells (Fig. 4C). Co-immunoprecipitation experiments using an anti-Myc antibody also demonstrated an association between Myc-MSR1 and HCV RNA in HCV-infected Myc-MSR1 cells (Fig. 4D, lane 3).

Collectively, the results shown in Figs. 3 and 4 demonstrate that MSR1 plays an essential role in the transport of double-stranded HCV RNA to TLR3, which engages this ligand in endosomes [4,11,12] to initiate signaling triggered by HCV infection.

A positively-charged region within the collagen superfamily domain of MSR1 is required for TLR3 signaling

The domain architecture of MSR1 (Fig. 5A) includes a conserved collagen superfamily domain with approximately 20 Gly-X-Y repeats that are predicted to form a collagen-like, triple-helical structure [34] (Fig. 5A). This domain is required for the binding of acetylated LDL to the bovine homolog of MSR1 [29], but its role in MSR1 recognition of dsRNA is unknown. We postulated that a series of positively-charged residues located within the carboxy terminus of the collagen superfamily domain, between amino acids (a.a.) 325–338 of human MSR1, could provide for interactions with the negatively-charged sugar-phosphate backbone of dsRNA, and thus be important for MSR1-mediated transport of dsRNA to TLR3. To test this hypothesis, we constructed a series of Myc-MSR1 expression vectors with deletion of a.a. 321–339 (Myc-MSR1/ Δ 321–339), or

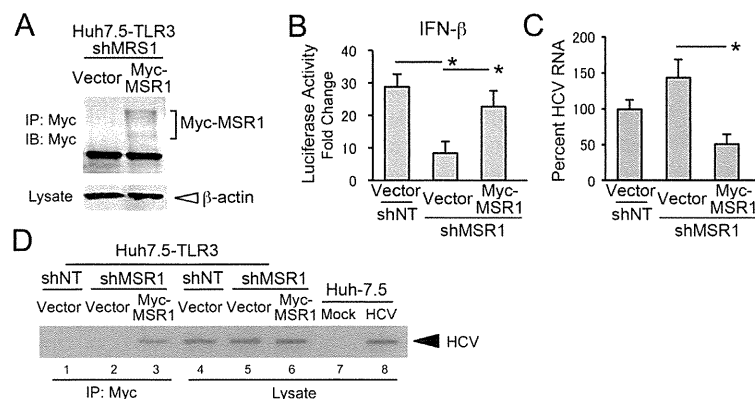


Figure 4. Reconstitution of MSR1 expression in MSR1-depleted cells restores TLR3 signaling triggered by HCV. (A) Reconstitution of MSR1 expression in Huh7.5-TLR3/shMSR1 cells. Myc-tagged MSR1 was stably expressed by retroviral transfer of a shMSR1-resistant vector (pCX4bsr/Myc-MSR1). Lysates were immunoprecipitated with anti-Myc, then subjected to immunoblotting as described in Materials and Methods. "Vector" = cells transduced with empty vector. (B) Restoration of poly(I:C) induction of IFN- β promoter activity by ectopically expressed Myc-MSR1 in Huh7.5-TLR3/shMSR1 cells. Cells were co-transfected with pCX4bsr/Myc-MSR1 (vs. empty vector), pIFN- β -Luc and pRL-CMV (internal control reporter) and cultured for 24 h, then treated with poly(I:C) (50 μ g/ml) for 6 hrs prior to lysis and luciferase assay. Huh7.5-TLR3/shNT cells, transfected with empty vector, were included as a positive control. (C) Quantitative RT-PCR analysis of HCV RNA in Huh7.5-TLR3/shMSR1 cells stably expressing Myc-MSR1 (vs. empty vector) 72 hrs after infection with HJ3-5 virus at an m.o.i. of 1. (D) Co-immunoprecipitation of HCV RNA with Myc-MSR1 in lysates of Huh7.5-TLR3/shMSR1 cells stably expressing Myc-MSR1 (lanes 3 and 6) vs. empty vector (lanes 2 and 5). Cells were infected with HJ3-5 virus (m.o.i. = 1) 72 hrs prior to lysis. Immunoprecipitation was with anti-Myc, demonstrating association of HCV RNA with Myc-MSR1. See legend to Fig. 1E for further details.

doi:10.1371/journal.ppat.1003345.g004

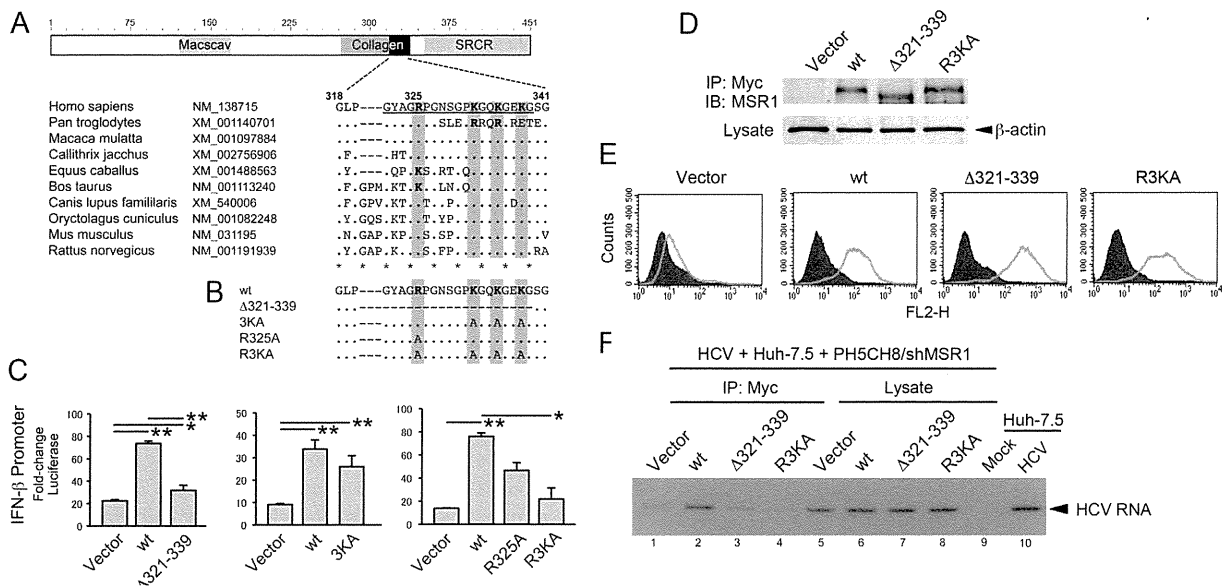


Figure 5. Poly(I:C) induced TLR3 signaling is dependent upon a conserved collagen superfamily domain in MSR1. (A) (top) Domain architecture of the 451 a.a. human MSR1 protein showing the location of the collagen superfamily domain that contains multiple G-X-Y repeats that form a triple helix [58]. (bottom) Alignment of human MSR1 with other mammalian MSR1 proteins near the C-terminus of the collagen domain, showing multiple conserved basic residues. GenBank accession numbers are shown for each. “Macscav” = conserved macrophage scavenger receptor domain; “SRCR” = Cys-rich scavenger receptor superfamily domain. (B) Myc-MSR1 mutants constructed within the pCX4bsr/Myc-MSR1 plasmid. (C) Poly(I:C) stimulated IFN- β promoter activity in MSR1-depleted Huh7.5 TLR3/shMSR1 cells transiently expressing wt or mutant Myc-MSR1: (left) Myc-MSR1/ Δ 321–339 (deletion of underlined sequence in panel A), (center) Myc-MSR1/3KA, or (right) Myc-MSR1/R325A and Myc-MSR1/R3KA. Cells were co-transfected with Myc-MSR1 expression vectors, pIFN- β -Luc and pRL-CMV (internal control), cultured for 24 h, then treated with poly(I:C) (50 μ g/ml) for 6 hrs before to lysis and luciferase assay. (D) Immunoblots showing expression of wt Myc-MSR1 and related mutants in PH5CH8/shMSR1 cells. Lysates were precipitated with anti-Myc antibody prior to anti-Myc immunoblot. (E) Flow cytometry histograms showing expression of Myc-MSR1 (wt) and indicated mutants on the surface of PH5CH8 cells (green lines). Purple curves indicate cell-surface staining with isotype immunoglobulins. “FL2-H” = fluorescent intensity. (F) Co-immunoprecipitation analysis of the association of HCV RNA with wt versus mutant Myc-MSR1 proteins in PH5CH8/shMSR1 cells co-cultured with Huh7.5 cells infected with HJ3-5 virus (m.o.i. = 1) for 72 hrs. RNA was extracted anti-Myc precipitates from lysates of co-cultures of infected Huh7.5 cells and PH5CH8/shMSR1 cells stably transduced with empty vector (lane 1 and 5), wt Myc-MSR1 (lane 2 and 6), Δ 321–339 (lane 3 and 7), or R3KA (lane 4 and 8). See legend to Fig. 1E for further details. doi:10.1371/journal.ppat.1003345.g005

alanine substitutions at one or more of the following positively-charged residues: Arg³²⁵, Lys³³², Lys³³⁵ and Lys³³⁸ (Fig. 5B). With the exception of Lys³³⁸, that is Glu in the chimpanzee (*Pan troglodytes*), a positively-charged side chain is conserved at each of these positions in MSR1 homologs from a wide variety of mammalian species (Fig. 5A). Consistent with an essential role for the carboxy terminus of the collagen superfamily domain in dsRNA trafficking, transient expression of Myc-MSR1/ Δ 321–339 failed to rescue poly(I:C) induction of IFN- β promoter activity in the MSR1-depleted Huh7.5-TLR3/shMSR1 cells (Fig. 5C, left panel). While Ala substitutions at Lys³³², Lys³³⁵ and Lys³³⁸ (Myc-MSR1/3KA) or at Arg³²⁵ (Myc-MSR1/R325A) caused only a modest reduction in the ability of the wt Myc-MSR1 to rescue signaling (Fig. 5C, center and right panels), Ala substitutions at all 4 positions (Myc-MSR1/R3KA) resulted in a nearly complete loss of the ability to rescue signaling in Huh7.5-TLR3/shMSR1 cells exposed to poly(I:C) (Fig. 5C, right panel). The mutants were expressed at high levels (Fig. 5D), and flow cytometry indicated that the Myc-MSR1/R3KA and Myc-MSR1/ Δ 321–229 mutants traffic to the cell surface (Fig. 5E). Thus, the loss of signaling cannot be explained by the MSR1 mutants being improperly processed, aberrantly degraded, or not transported to the cell surface. The results are consistent with a loss of dsRNA-binding capacity by Myc-MSR1/ Δ 321–339 and Myc-MSR1/R3KA, and suggest that the positively-charged residues in the MSR1 collagen superfamily domain are involved in dsRNA transport and required for TLR3 signaling.

To confirm that these mutations do in fact ablate the ability of MSR1 to bind HCV RNA replication intermediates, we assessed the association of wt Myc-MSR1, Myc-MSR1/ Δ 321–339 and Myc-MSR1/R3KA with HCV RNA in co-immunoprecipitation experiments (Fig. 5F). HJ3-5 virus-infected Huh-7.5 cells were co-cultured with MSR1-depleted PH5CH8/shMSR1 cells in which stable expression of each of these Myc-MSR1 mutants (or empty vector) had been established. Cell lysates were immunoprecipitated with anti-Myc antibody, and RNA extracted from the immunoprecipitates assayed by HCV-specific RT-PCR. The anti-Myc immunoprecipitate prepared from cells expressing wt Myc-MSR1 was significantly enriched in HCV RNA (Fig. 5F, lane 2) compared to immunoprecipitates prepared from cells expressing either the Δ 321–339 or R3KA mutants (lanes 3 and 4), or empty vector (lane 1). Collectively, these results reveal that conserved positively-charged residues within the carboxy terminus of the collagen superfamily domain of MSR1 are essential for TLR3-mediated responses to dsRNA, and that they contribute to a dsRNA-binding domain in MSR1.

MSR1 facilitates TLR3 recognition of HCV infection in neighboring cells

Since infected Huh-7.5 cells served as the source of viral RNA bound by Myc-MSR1 expressed within the PH5CH8/shMSR1 cells in the co-culture experiment shown in Fig. 5, these results suggest that TLR3, through the dsRNA-scavenging functions of MSR1, is capable of sensing the presence of HCV infection in

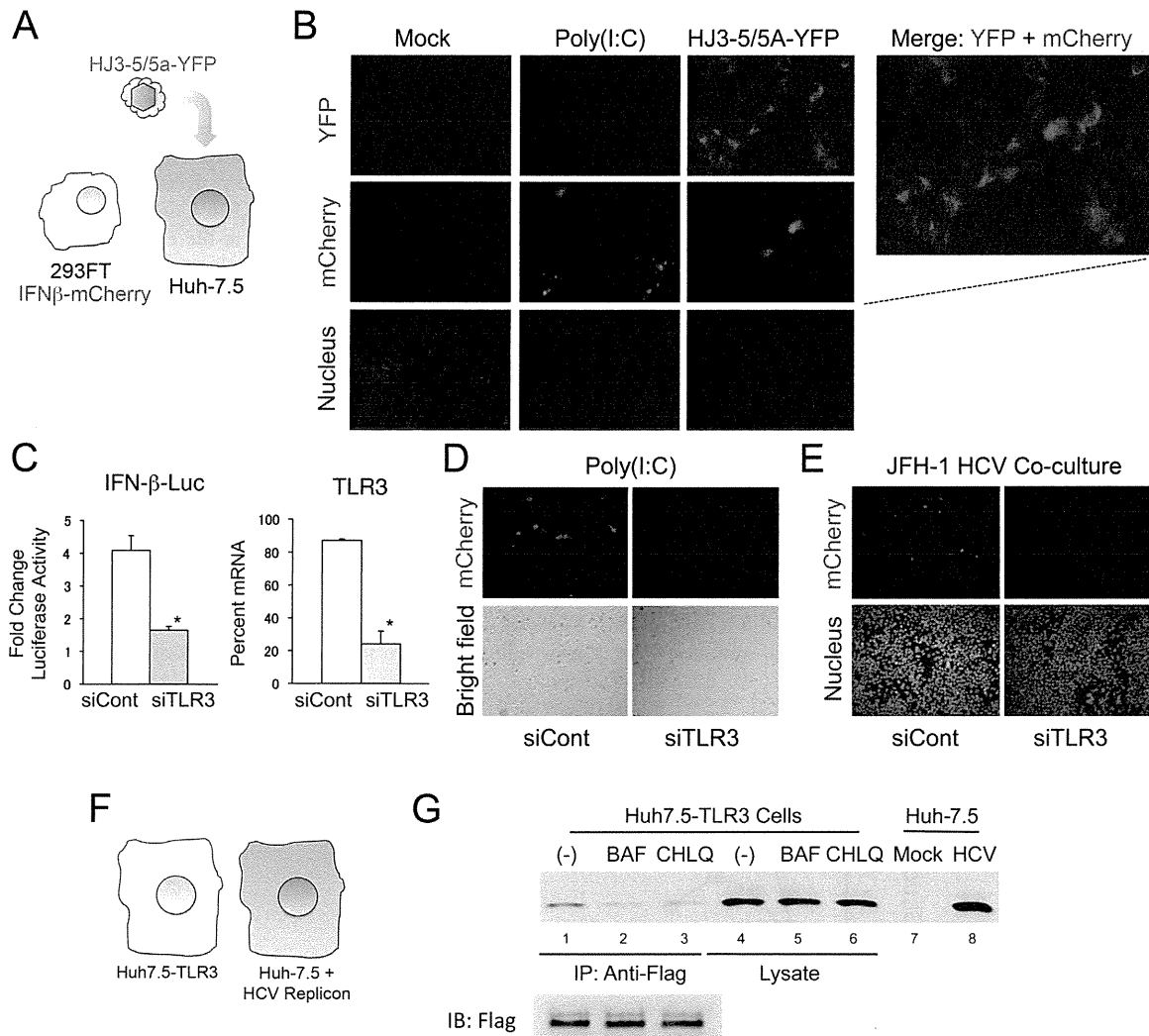


Figure 6. TLR3 expressed in 293-hTLR3 cells senses HCV replication in adjacent human hepatocytes. (A) Experimental design, showing co-culture of HCV-nonpermissive, TLR3-competent 293FT/IFN- β -mCherry cells expressing mCherry under control of the IFN- β promoter with Huh-7.5 cells that are HCV permissive and TLR3 incompetent. Cells were infected with HJ3-5/5A-YFP virus that expresses YFP as a fusion with NS5A. (B) Immunofluorescence microscopy demonstrating induction of mCherry expression in 293FT/IFN- β -mCherry + Huh-7.5 cell co-cultures upon stimulation with poly(I:C) or infection with HJ3-5/NS5A-YFP virus. HCV replication was visualized by YFP expression and present in cells adjacent to those expressing mCherry in the two-color merged images at the far right. Nuclei were visualized by DAPI counterstain. (C) siRNA-mediated depletion of TLR3 significantly reduces poly(I:C)-induced activation of the IFN- β promoter in 293FT/IFN- β -mCherry cells. (left) Fold-change in luciferase activity induced by extracellular poly(I:C) in 293FT/IFN- β -mCherry cells transfected with TLR3-specific (siTLR3) or control (siCont) siRNAs. The cells were transfected with an IFN- β -Luc reporter plasmid. * $p \leq 0.02$. (right) qRT-PCR detection of TLR3-specific mRNA in cells transfected with the siTLR3 or siCont siRNAs. * $p \leq 0.02$. (D) Poly(I:C)-induced expression of mCherry in 293FT/IFN- β -mCherry cells is ablated by prior transfection with TLR3-specific siRNA. (E) siRNA-mediated depletion of TLR3 eliminates mCherry expression by 293FT/IFN- β -mCherry cells placed in co-culture with HCV-infected Huh-7.5 cells. 293FT/IFN- β -mCherry cells were transfected with siTLR3 or siCont siRNAs 3 days prior to being placed in co-culture with Huh-7.5 cells infected with genotype 2a JFH-1 virus. (F) Experimental design, showing Huh7.5-TLR3 cells co-cultured with Huh7.5 cells supporting replication of a genome-length genotype 1a HCV RNA replicon. (G) Co-immunoprecipitation analysis of the association of HCV RNA with Flag-TLR3 in co-cultures of Huh7.5-TLR3 and HCV replicon cells (panel F) after treatment with bafilomycin (1.0 nM, lanes 2 and 5) or chloroquine (5.0 μ M, lanes 3 and 6) for 72 hrs. RNA was extracted from anti-Flag precipitates prepared from lysates of the co-cultured cells and subjected to HCV-specific RT-PCR. See legend to Fig. 1E for further details.
doi:10.1371/journal.ppat.1003345.g006

adjacent cells. This is an important observation, as previous studies demonstrating TLR3 sensing of HCV infection by hepatocytes [4] have not distinguished between the sensing of replication intermediates produced within the same cell versus those released into the extracellular milieu from neighboring infected cells.

To further explore this phenomenon, we generated cell lines that could serve as either infected “inducer” cells or TLR3-competent “sensor” cells in co-culture experiments (Fig. 6A). The

inducer cells were Huh-7.5 cells infected with HJ3-5/5A-YFP virus, which expresses a fusion of the NS5A protein with YFP [35], thereby allowing infected cells to be identified by fluorescence microscopy. These inducer cells are not competent for either RIG-I or TLR3 signaling [17,26]. The sensor cells were 293FT/IFN- β -mCherry cells, human embryonic kidney cells expressing endogenous TLR3 and the fluorescent reporter protein, mCherry, under the control of the IFN- β promoter. These 293FT/IFN- β -mCherry

cells express a low, but readily detectable level of MSR1 transcripts (Fig. 2B, lower panel). Importantly, they are nonpermissive for HCV replication. As expected, co-culture of mock-infected Huh-7.5 cells and the 293FT/IFN- β -mCherry cells resulted in no detectable YFP or mCherry signal (Fig. 6B, left set of panels). However, mCherry expression could be induced by the addition of poly(I:C) to the medium bathing these co-cultured cells (Fig. 6B, second set of panels from the left). Infection of the co-cultured cells with HJ3-5/5A-YFP virus also resulted in the induction of mCherry in the 293FT/IFN- β -mCherry cells (Fig. 6B, right panels and merged image). The cells expressing mCherry lacked detectable YFP fluorescence, confirming that they were not infected. Similar results were obtained with 293/hTLR3-IFN- β -mCherry cells, which are engineered to overexpress TLR3, and also express mCherry under control of the IFN- β promoter (Supplementary Fig. S3). Prior transfection of 293FT/IFN- β -mCherry cells with siRNA targeting TLR3 significantly reduced poly(I:C)-induced IFN- β promoter activity (Fig. 6C) and mCherry expression (Fig. 6D), confirming that dsRNA sensing by TLR3 activates the IFN- β promoter (and mCherry expression) in these cells. Similarly, siRNA-mediated depletion of TLR3 in 293FT/IFN- β -mCherry cells largely eliminated mCherry expression when the cells were co-cultured with HCV-infected Huh-7.5 cells (Fig. 6E). These results indicate that TLR3 is capable of sensing

HCV infection in neighboring cells, presumably via MSR1-mediated transport of extracellular dsRNA to the endosome where TLR3 is expressed.

In separate experiments, HCV RNA co-immunoprecipitated with Flag-TLR3 when Huh7-TLR3 cells were co-cultured with Huh-7.5 cells containing an HCV replicon RNA (Fig. 6F and G), providing additional evidence that HCV RNA produced in adjacent cells may serve as ligand for TLR3. Consistent with the fact that TLR3 signaling is initiated only in the endosome, not at the cell surface [12], and more specifically that acidification of the endosome is required for TLR3 signaling in Huh7.5-TLR3 cells [4], treatment of these co-cultured cells with bafilomycin (1 nM) or chloroquine (5 μ M) substantially reduced the amount of HCV RNA that co-immunoprecipitated with TLR3 (Fig. 6G).

To demonstrate that TLR3 signaling induced within cells adjacent to those infected results in functional antiviral activity, as well as to formally demonstrate a role for MSR1 in this process, we replaced the 293 sensor cells with PH5CH8 cells (Fig. 7A, left). These T antigen-transformed, TLR3-competent human hepatocytes [17] are nonpermissive for HCV infection due in part to a lack of expression of miR-122 (D. Yamane and S.M. Lemon, unpublished data), an essential host factor for HCV replication [36]. We infected Huh-7.5 cells with HJ3-5/GLuc2A virus, and 6 hrs later split the culture to create co-cultures of HCV-infected

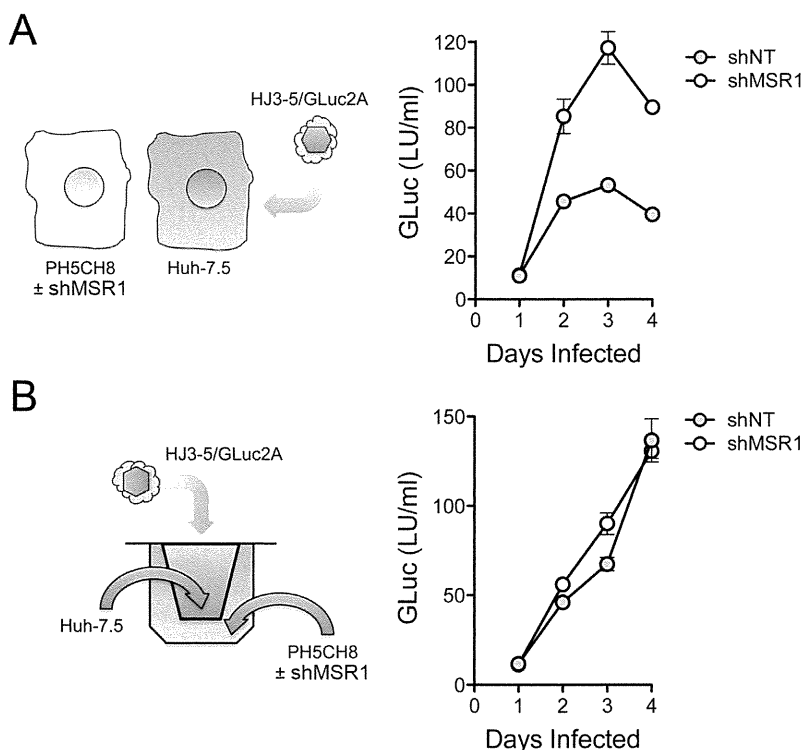


Figure 7. MSR1-dependent TLR3 sensing of HCV infection in neighboring cells restricts viral replication. (A) (left) Design of co-culture experiments in which HCV-nonpermissive, but TLR3-competent, PH5CH8 cells were co-cultured with HCV-permissive, but RIG-I and TLR3-incompetent, Huh-7.5 cells infected with HJ3-5/GLuc2A, a reporter virus that expresses GLuc as a component of its polyprotein. Huh-7.5 cells were infected with virus for 6 hrs prior to being split and added to either MSR1-depleted PH5CH8/shMSR1 or control PH5CH8/shNT cells (Fig. 3A) at a ratio of 1:2 to establish co-cultures. (right) *Gaussia* luciferase activity in supernatant fluids of HJ3-5/GLuc2A-infected co-cultures. Data shown are means \pm s.d. from 3 replicate cultures and are representative of repeat, independent experiments. The difference in GLuc expression from shMSR1- vs. shNT-treated cells was significant by two-way ANOVA ($p < 0.0001$). (B) (left) Co-cultures of PH5CH8/shMSR1 (or control PH5CH8/shNT) cells and HJ3-5/GLuc2A virus-infected Huh-7.5 cells in which the cell types are separated by a semi-permeable membrane (Transwell system). (right) *Gaussia* luciferase activity in supernatant fluids of HJ3-5/GLuc2A virus-infected Huh-7.5 cells separated from the PH5CH8 cells by a semi-permeable membrane. Data shown are means \pm s.d. from 3 replicate cultures. Unlike Huh-7.5 cells cultured in close continuity with PH5CH8 cells (panel A), there is no restriction to HCV replication when the cell types are separated by a permeable membrane. The difference in GLuc expression from shMSR1- vs. shNT-treated cells was not significant by two-way ANOVA ($p = 0.20$).

doi:10.1371/journal.ppat.1003345.g007

Huh-7.5 cells and either MSR1-depleted PH5CH8 cells or PH5CH8 cells transduced with the non-targeting control, shNT (Fig. 2A). HCV replication in the co-cultures was monitored over time by measuring GLuc activity in the culture supernatant fluids (Fig. 7A, right). Our expectation was that TLR3-dependent signaling should be triggered in PH5CH8 cells when placed in co-culture with infected Huh-7.5 cells (that lack both TLR3 and RIG-I-mediated signaling) [17,26], and that this would result in an antiviral response capable of restricting HCV replication in the Huh-7.5 cells through paracrine signaling. This was precisely what we observed. Secreted GLuc activity, which is proportionate to the replication of the reporter virus, was consistently reduced by 50% or more when the infected cells were co-cultured with PH5CH8/shNT versus PH5CH8/shMSR1 cells (Fig. 7A, right). Since some laboratory strains of HCV induce apoptosis in Huh-7.5 cells [37], we determined the proportion of Huh-7.5 cells undergoing apoptosis after 4 days of infection with HJ3-5/GLuc2A virus. These studies demonstrated no increase in the proportion of Huh-7.5 cells expressing detectable cleaved caspase 3 protein or demonstrating TUNEL fluorescence (Supplementary Fig. S4). Thus, apoptosis of infected cells is not required for sensing of infection by adjacent, TLR3 competent hepatocytes.

To gain further insight into the MSR1-mediated restriction of HCV replication in neighboring cells, we assessed the replication of HJ3-5/GLuc2A virus in Huh-7.5 cells that were separated from PH5CH8/shMSR1 (or PH5CH8/shNT) cells by a permeable membrane in Transwell culture dishes (Fig. 7B, left). Under these conditions, MSR1 depletion in the TLR3-competent PH5CH8 cells had no impact on the rate of HCV replication in the Huh-7.5 cells (Fig. 7B, right). These results indicate a need for close positioning and possibly direct cell-cell contact for MSR1-dependent sensing of infection in neighboring hepatocytes. Despite the restriction imposed on virus replication in Huh-7.5 cells by PH5CH8 cells, we were unable to detect IFN- β in media from the direct co-cultures (Fig. 7A) using an ELISA with a level of detection of approximately 10 pg/ml. Collectively, these data show that the antiviral response induced by MSR1-dependent recognition of viral RNA produced in neighboring cells is functional and restricts replication in the infected cell, but that this effect is limited in magnitude and highly localized.

Discussion

The class A scavenger receptors comprise a diverse family of 5 homotrimeric, single-pass type II membrane proteins that bind to and facilitate the cellular import of a broad range of ligands, including acetylated LDL, bacterial cell wall constituents, and both ssRNA and dsRNA [20,22,32]. While their expression has been considered previously to be restricted to cells of myeloid origin, primarily macrophages (hence the name, “macrophage scavenger receptor”), more recent data suggest that members of this receptor family are expressed more ubiquitously and are present on the surface of a variety of cell types [22]. The various members of the family differ in length, domain architecture, ligand specificity and function, but have been recognized increasingly to play important roles in innate immune signaling. Several class A scavenger receptors, in particular MARCO (or SCARA2), and SCARA4 (collectin-12), function in innate immune recognition of bacterial infections, while MSR1 (SCARA1, SR-AI, or CD204) has been shown recently to contribute to antiviral responses evoked by extracellular dsRNA [reviewed in 22]. Mice with genetic deficiency of the homolog of MSR1 demonstrate increased susceptibility to infection with herpes simplex virus [38], while

MSR1 is required for induction of TLR3-mediated signaling in monocytes exposed to human cytomegalovirus [39].

DeWitte-Orr et al. [22] have recently suggested that the family of class A scavenger receptors represent the major receptors for dsRNA on the surface of fibroblasts, and that they act in a cooperative fashion to deliver dsRNA to both endosomal TLR3 as well as RIG-I-like helicases expressed within the cytoplasm of these cells. The data we present here provide additional support for this general conclusion, but show with greater specificity that MSR1 is the dominant surface receptor for dsRNA in human hepatocyte-derived cell lines. While DeWitte-Orr et al. [22] found that selective knockdown of any one member of the class A scavenger receptor family (including MSR1) had no effect on dsRNA uptake or poly(I:C)-stimulated ISG expression, we found that a relatively low efficiency knockdown of MSR1 only profoundly disrupts the ability of extracellular poly(I:C) to stimulate IFN- β promoter activity and ISG expression in both Huh7.5-TLR3 cells and PH5CH8 cells (Fig. 3). In all of our studies, these two cell lines behaved similarly. This is important, as Huh-7 cells, from which Huh7.5-TLR3 cells are derived, originate from an hepatocellular carcinoma. In contrast, the PH5CH8 cell line was established by transformation of non-neoplastic human hepatocytes with the large T antigen of simian virus 40 [30]. These cells, like primary hepatocytes, express TLR3 endogenously and are stimulated to produce an IFN response when exposed to extracellular poly(I:C) [4]. Although hepatocytes express several members of the class A scavenger receptor family (Fig. 2), the fact that depletion of MSR1 alone disrupts this response suggests that MSR1 is uniquely required for the uptake and transport of extracellular dsRNA so that it may be sensed by TLR3 in these cells.

In addition to showing that MSR1 expression is required for TLR3-mediated responses to poly(I:C) or infectious challenge with HCV in hepatocyte-derived cells, our data show that MSR1 is physically associated with viral RNA, even when it is produced by ongoing RNA replication in neighboring cells (Fig. 6F and G), and that MSR1 expression is required for TLR3 to bind HCV RNA as ligand (Fig. 3J). We show directly that MSR1 forms a complex with HCV RNA (Fig. 4D), and identify several conserved basic residues within the carboxyl terminus of the collagen superfamily domain that are required for dsRNA uptake by MSR1 and TLR3-mediated signaling in hepatocytes (Fig. 5). There are three alternatively spliced isoforms of MSR1 in humans, only two of which (type I and type II) are expressed on the plasma membrane and facilitate endocytosis of ligands [40]. While the type I isoform is 451 a.a. in length, type II MSR1 is only 358 a.a. However, the amino-terminal 343 residues of these isoforms are identical in sequence, and both isoforms contain the collagen superfamily domain and RNA-binding subdomain we have identified between residues 321–339. Importantly, although we found a low abundance of isoform II transcripts in Huh-7.5 cells (Fig. 2B), only isoform I (49.7 kDa) was detected in immunoblots of Huh7.5-TLR3 and PH5CH8 cells, and not isoform II (39.6 kDa) or III (42.9 kDa).

The positively-charged carboxy-terminal region of the collagen superfamily domain is required for the association of MSR1 with acetylated LDL [41]. Its sequence is highly conserved among mammalian species with the exception, interestingly, of the chimpanzee (Fig. 5A). In addition to the 4 positively charged residues (Arg³²⁵, Lys³³², Lys³³⁵ and Lys³³⁸) present in human MSR1, this subdomain contains a conserved negatively-charged residue (Glu³³⁷). Previous studies suggest this domain assumes a collagen-like, triple-helical conformation at pH>4.5, stabilized in part by electrostatic interactions of Glu³³⁷ with one of the conserved Lys residues [34]. This leaves the remaining unpaired

basic residues available for intermolecular interactions with ligands, including association with the negatively-charged sugar-phosphate backbone of dsRNA. MSR1 bound to acetylated LDL is internalized through receptor-mediated endocytosis, dissociating under acidic conditions within the endosome due to the loss of ion pairing between Glu³³⁷ and the conserved Lys residues within the collagen-like domain [34,42]. We presume that MSR1 functions similarly in the uptake of dsRNA from the extracellular milieu. This may explain why inhibitors of endosomal acidification block TLR3-mediated antiviral responses, as we have shown previously for Huh7.5-TLR3 cells [4], and inhibit the co-immunoprecipitation of HCV RNA with TLR3 in infected Huh7.5-TLR3 cells (Fig. 6D).

An important observation to emerge from these studies is that hepatocytes are capable of sensing HCV infection in adjacent cells, and that MSR1 mediates this response by acting as a carrier of replication intermediates (presumably dsRNA) from the extracellular milieu to endosomally expressed TLR in uninfected cells. While it is often assumed that TLR3 expressed within parenchymal cells such as hepatocytes may sense virus infection in neighboring cells, we demonstrated this formally in co-cultures of HCV-nonpermissive, TLR3-competent cells (293FT or PH5CH8 cells) and infected Huh-7.5 cells that are deficient in both TLR3 and RIG-I sensing of HCV infection [17,26] (Figs. 6 and 7). We show that this results in a localized antiviral effect, restricting the replication of virus in the co-cultured cells, and that it is dependent upon MSR1 expression in the uninfected cells since it can be blocked by RNAi-mediated depletion of MSR1 (Fig. 7B).

These observations have important implications for the pathogenesis of chronic hepatitis C. For reasons that are unclear, only a small fraction of hepatocytes appear to be infected with HCV in these patients [25]. Two-photon immunofluorescence microscopy of frozen sections of infected human liver tissue has revealed clusters of infected cells, identified either by detection of HCV-specific antigens or dsRNA replication intermediates, typically surrounded by greater numbers of uninfected cells [25]. The presence of these discreet foci of infection suggests that the spread of virus is actively restricted within the liver. The data we present here suggest a model in which TLR3 mediates the establishment of an antiviral state in uninfected cells adjacent to those that are infected in a process that is facilitated by the dsRNA-scavenging actions of MSR1. Such a model also explains why HCV infection induces ISG expression within the liver, despite its ability to disrupt both RIG-I and TLR3 responses by NS3/4A-mediated cleavage of the RIG-I adaptor molecule, MAVS [15,16], and the TLR3 adaptor molecule, TICAM-1 (TRIF), within infected cells [4,18]. TLR3 sensing of HCV infection is not likely to be restricted to neighboring hepatocytes, as we have demonstrated here, but may also occur in tissue-resident macrophages (Kupffer cells) or monocyte-macrophages recruited to the site of infection. TLR7 expressed within plasmacytoid dendritic cells (pDCs) may also sense infection in other cells [43]. While less robust on a single cell level than in these “professional” innate immune cells, TLR3-mediated antiviral responses in the very large number of parenchymal hepatocytes exposed to HCV may nonetheless make a substantial contribution overall to the induction of intrahepatic ISG responses observed in patients with chronic hepatitis C [24].

Materials and Methods

Cells

Huh-7.5 cells [44] were a gift from Charles Rice (Rockefeller University, NY). Huh-7.5 cells engineered to express either TLR3

or the TLR3 mutants Δ IR, H539E or N541A have been described previously [4]. 293FT cells, human embryonic kidney cells transformed with SV40 T antigen, were purchased from Invitrogen (Carlsbad, CA). 293-hTLR3 cells (engineered to over-express human TLR3) were purchased from InvivoGen. The non-neoplastic T-antigen immortalized hepatocyte cell line PH5CH8 has been described previously [30,45]. These cells were cultured in Dulbecco’s modified Eagle’s medium (Invitrogen) supplemented with 10% fetal bovine serum. Blasticidin (2 μ g/ml) or G418 (0.3 mg/ml) was added for the selection of cells exogenously expressing TLR3-Flag, Myc-MSR1 and related mutants. G418 (0.3 mg/ml) was added for the selection of HCV RNA replicon colonies.

Virus

Two strains of HCV were used in these studies: the genotype 2a JFH-1 virus [46], and HJ3-5, a cell culture-adapted genotype 1a/2a chimeric virus containing the structural proteins of the genotype 1a H77 virus placed within the background of JFH-1 virus [47,48]. HJ3-5/GLuc2A is a derivative of HJ3-5 containing the *Gaussia princeps* luciferase (GLuc) coding sequence fused to the foot-and-mouth disease virus (FMDV) 2A sequence and inserted between p7 and NS2 of HJ3-5 virus [49]. Cells were infected at an m.o.i. of 1. GLuc activity in supernatants was measured by BioLux *Gaussia* Luciferase Assay Kit (New England Biolabs, Ipswich, MA) using a Synergy2 multi-mode microplate reader (BioTek, Winooski, VT). HJ3-5/5A-YFP is another derivative of HJ3-5 containing yellow fluorescent protein (YFP) coding sequence fused to NS5A sequence [35].

Plasmids

ptat2ANeoH77S [27] contains the *tat* protein, 15 amino acids of the FMDV 2A protein and neomycin phosphotransferase (Neo^R) downstream of HCV internal ribosome entry site (IRES) and the full-length H77S (genotype 1a) polyprotein-coding sequence downstream of the encephalomyocarditis virus IRES. pIFN- β -Luc and pPRDII-Luc have been described previously [50,51]. pIFN- β -mCherry, which expresses the mCherry fluorescent protein under transcriptional control of the IFN- β promoter, was constructed by replacing the firefly luciferase sequence in pIFN- β -Luc with the mCherry sequence. pJFH1-T3 was constructed by introducing a T3 promoter downstream of the HCV 3’UTR in pJFH1 [46].

pCX4neo/Myc-MSR1 and pCX4bsr/Myc-MSR1 were constructed from the retroviral vectors pCX4neo and pCX4br [52], which contain the resistance gene for neomycin and blasticidin respectively. A DNA fragment encoding MSR1 (accession no. NM_138715) was amplified from cDNA obtained from Huh-7 cell DNA by PCR using PrimeSTAR HS DNA polymerase (TaKaRa) and primers with *Sph*I (forward) and the *Not*I (reverse) recognition sites that were designed to enable expression of the MSR1 ORF. The DNA was cloned into the *Sph*I and *Not*I sites of pCX4neo/Myc and pCX4bsr/Myc, fusing MSR1 sequence to Myc. Mutations within the Myc-MSR1 sequence were subsequently constructed by PCR mutagenesis as previously described [53]. The nucleotide sequences of these vectors were confirmed by DNA sequencing. Cells stably expressing Myc-MSR1 were prepared as previously described [54].

Synthetic HCV dsRNA

pJFH1-T3 was linearized by either *Xba*I or *Eco*RI to provide templates for synthesis of positive- or negative-stranded HCV RNA using T7 or T3 MEGAscript kits (Ambion, Austin, TX). Positive- and negative-stranded HCV RNA products were

annealed to produce dsRNA by heating at 70°C for 10 minutes followed by slow cooling to room temperature. The annealed product was assayed for sensitivity to S1 nuclease (Promega, Madison, WI) to confirm that it was double-stranded.

Poly(I:C)

High molecular weight (HMW) poly(I:C) was purchased from Invivogen (San Diego, CA). Cells were exposed to a concentration of 50 µg/ml for 6 hrs unless otherwise stated. Fluorescein-labeled HMW poly(I:C) (Invivogen) was used to monitor dsRNA uptake by cells. Cells were mock-exposed or exposed to 10 µg/ml fluorescein-labeled poly (I:C) for 8, 16 or 24 hrs, then harvested by trypsinization, washed twice in phosphate buffered saline (PBS) and fixed for 15 minutes in 4% paraformaldehyde. After additional washing in 1× PBS, the fluorescence intensity of cell populations was analyzed using a Beckman Coulter (Dako) CyAn flow cytometer.

Promoter reporter assays

IFN-β and NF-κB-dependent promoter activities were assayed using firefly luciferase reporters, pIFN-β-Luc or pPRDII-Luc, with the reporter plasmid pRL-CMV used as an internal control for transfection efficiency as previously described [55]. A Turner Designs Luminometer Model TD-20/20 (Promega, Madison, WI) was used to measure luciferase activity. Data shown represent means ± s.d. from three independent transfection experiments.

Immunoblot analysis

Preparation of cell lysates and SDS-PAGE were carried out as previously described [56]. Total protein was transferred to Immobilon-psq PVDF membranes (Millipore, Billerica, MA) using a Trans-blot SD semi-dry transfer cell (Bio-Rad, Hercules, CA). Primary antibodies included anti-Flag (M2; Sigma, St Louis, MO), anti-Myc (9B11; Cell Signaling, Danvers, MA), anti-ISG15 (H-150; Santa Cruz Biotechnology Inc., Santa Cruz, CA), anti-MSR1 (H-190; Santa Cruz Biotechnology Inc.), and anti-β-actin antibody (AC-15; Sigma). Secondary antibodies were IRDye-conjugated anti-mouse IgG and anti-rabbit IgG (LI-COR Biosciences, Lincoln, NE). Immunocomplexes were detected with an Odyssey infrared imaging system (LI-COR Biosciences).

Quantitative RT-PCR analysis

Total cellular RNA was isolated using the RNeasy mini kit (Qiagen, Valencia, CA). The iScript one-step RT-PCR kit with SYBR Green and CFX96 real-time system (Bio-Rad) were used to quantify the abundance of IFN-β, ISG56, GAPDH mRNA or HCV RNA. We used the following forward and reverse primer sets: IFN-β, 5'-GTGCCTGGACCATAGTCAGAGTGG-3' (forward), 5'-TGTCAGTCCCAGAGGCACAGG-3' (reverse); ISG56, AAGCTTGAGCCTCCTTGGGTTTCGT-3' (forward), 5'-TCAAAGTCAGCAGCCAGTCTCAGG-3' (reverse); GAPDH [53], HCV, 5'-CATGGCGTTAGTATGAGTGTTCGT-3' (forward), 5'-CCCTATCAGGCAGTACCACAA-3' (reverse). IFN-β, ISG56 and HCV RNAs were normalized to GAPDH mRNA. Results shown represent means ± s.d. from three independent experiments.

Co-immunoprecipitation of Flag-TLR3 or Myc-MSR1 with HCV RNA

Total cell lysates were prepared using lysis buffer (PBS containing 0.2% Triton X-100, RNase inhibitor and protease inhibitor cocktail), followed by immunoprecipitation with anti-Flag or anti-Myc antibodies using protein G sepharose (GE healthcare).

RNAs were extracted from the immunoprecipitates using Trizol (Invitrogen), and assayed for HCV RNA by RT-PCR using the Superscript III One-step RT-PCR system (Invitrogen) followed by agarose gel electrophoresis.

MSR1-depleted cells and Myc-MSR1 expression

Short hairpin RNA (shRNA) targeting MSR1 (shMSR1, 5'-GCATTGATGAGAGTGCTATTG-3') or non-targeting control shRNA (Sigma; Mission shRNA SHC-002) were introduced into Huh7.5-TLR3 or PH5CH8 cells by lentiviral transfer. MSR1-depleted Huh7.5-TLR3/shMSR1 and PH5CH8/shMSR1 and related control cells, Huh7.5-TLR3/shNT or PH5CH8/shNT cells, were selected by addition of puromycin (5 µg/ml) to the cell culture medium. MSR1 expression was reconstituted in MSR1-depleted cells by retroviral transfer of the Myc-MSR1 sequence in pCX4neo Myc-MSR1, which lacks the shMSR1 target sequence within the 5'UTR of MSR1 mRNA [57]. Cells stably expressing Myc-MSR1 were selected by growth in G418 (0.3 mg/ml).

For analysis of the RNA-binding domain in MSR1, pCX4neo-Myc-MSR1 was subjected to PCR-based mutagenesis using standard methods, with the sequence of the manipulated regions of the plasmid confirmed by DNA sequencing. Cell surface expression of MSR1 and related mutants was analyzed by flow cytometry. MSR1 has a transmembrane domain between aa 51–73, with its carboxyl terminus exposed to the extracellular environment. For detection of MSR1 on the cell surface, non-permeabilized cells were fixed with 2% paraformaldehyde followed by incubation with anti-MSR1 antibody (Santacruz, H-190) for 1 h at room temperature. Cells were washed three times with PBS, and incubated with R-phycoerythrin-conjugated anti-rabbit IgG secondary antibody (Jackson ImmunoResearch) for 30 min at room temperature. Fluorescent intensity of cells was determined using a FACScan (Becton Dickinson) flow cytometer.

Measurements of apoptosis in infected cells

Huh-7.5 cells were infected with HJ3-5/GLuc2A virus at an m.o.i. of 0.03, or mock-infected, and cultured for 4 days. As a positive control, cells were treated with 1 µM staurosporine for 6 hrs. Cells were harvested by trypsinization, washed twice in PBS and fixed in 4% paraformaldehyde, then stained for cleaved caspase 3 and HCV core protein as described previously [37]. DNA fragmentation was analyzed by terminal deoxynucleotidyl-transferase-mediated dUTP-biotin nick end-labeling (TUNEL) system (Promega, Madison, WI). Positive cells were quantified by flow cytometry as described previously [37].

Statistical methods

Statistical comparisons were carried out using Student's T test unless otherwise noted. Calculations were made with Excel 2008 for Mac (Microsoft) or Prism V for Mac OS X (GraphPad Software).

Supporting Information

Figure S1 Replicon colony formation assay demonstrates that TLR3 expression restricts HCV replication.

Ten µg RNA, synthesized in vitro from linearized ptat2AneoH77S DNA using a T7 MEGAscript kit (Ambion), were electroporated into Huh7.5-TLR3, -ΔTIR, -H539E or -N541A cells in a 4-mm cuvette by pulsing once at 400 V, 250 µF, and infinite Ω in a BioRad Gene Pulser Xcell apparatus. The cells were then cultured in G418 (0.3 mg/ml) for 3 weeks, and surviving cell colonies stained with Coomassie brilliant blue (0.06% in 50% methanol-10% acetic acid).

(TIF)

Figure S2 TLR3 preferentially senses very high molecular weight poly(I:C). (A) To determine whether TLR3 discriminates between dsRNA of different lengths corresponding to the size of viral genomes, we studied two dsRNA surrogates, low-molecular weight (LMW) and high-molecular weight (HMW) poly(I:C), that are between 0.2–1.0 and 1.5–8 kilobase pairs, respectively. (B) Both LMW and HMW poly(I:C) stimulated IFN- β promoter activity in a dose-dependent manner when added to the medium bathing (left) Huh-7.5 cells engineered to express wt TLR3 (Huh7.5-TLR3 cells), but not (right) Huh7.5- Δ TIR cells that express a defective TLR3 lacking the TIR domain and thus incapable of signaling. Importantly, however, HMW poly(I:C) was 300-fold more active than LMW poly(I:C) on a molar basis in stimulating IFN- β promoter activity. (C) This was reflected in significantly greater induction of ISG56 mRNA expression by HMW vs. LMW poly(I:C) in Huh7.5-TLR3 cells or PH5CH8 cells that naturally express TLR3. (D) At comparable concentrations, HMW poly(I:C) was also more active than LMW poly(I:C) in stimulating ISG15 protein expression in Huh7.5-TLR3 cells. Note the absence of ISG15 expression induced by either poly(I:C) in Huh7.5-H539E cells that express an inactive TLR3 mutant that is defective in dsRNA binding. (E) Similar differences in poly(I:C) induction of ISG15 protein expression were observed in PH5CH8 cells. Note that ISG15 expression was reduced by shRNA knockdown of TLR3 in these cells. Collectively, these results suggest that very lengthy dsRNA, such as viral replication intermediates, are more powerful inducers of TLR3-mediated antiviral responses than dsRNAs under 1 kb in length. While the mechanistic basis of this is uncertain, one possibility is that the greater signaling strength derives from progressive recruitment of multiple TLR3 ectodomains aligned along a single dsRNA molecule. (TIF)

Figure S3 Induction of IFN- β promoter activity in 293-hTLR3/IFN- β -mCherry cells co-cultured with HCV-infected Huh-7.5 cells. (A) Human 293-hTLR3/IFN- β -mCherry cells transduced to overexpress TLR3 and the IFN- β -mCherry reporter were co-cultured with infected or uninfected Huh-7.5 cells using the same general experimental design as in the experiment shown in Fig. 6A in the main manuscript. (B) Immunofluorescence microscopy demonstrating induction of mCherry expression in 293-hTLR3/IFN- β -mCherry + Huh-7.5 cell co-cultures upon stimulation with poly(I:C) or infection with HJ3-5/NS5A-YFP virus. HCV replication was visualized by YFP expression and is observed in cells adjacent to those expressing mCherry in the two-color merged images at the bottom. Nuclei were visualized by DAPI counterstain. (TIF)

Figure S4 Absence of apoptosis in HJ3-5/GLuc2A-infected cells. Analysis of cleaved caspase 3 and HCV core protein (top row) and DNA fragmentation by TUNEL assay (bottom row) in Huh-7.5 cells at 4 d following mock infection or infection with HJ3-5/GLuc2A virus at a m.o.i. of 0.03. Cells treated with 1 μ M staurosporine for 3 hrs are shown as a positive control for apoptosis induction. (TIF)

Acknowledgments

The authors are grateful to Zongdi Feng for helpful advice and review of the manuscript, and to Cindy Hensley for expert technical assistance.

Author Contributions

Conceived and designed the experiments: HD DY CW DRM FH SML. Performed the experiments: HD DY DRM FH. Analyzed the data: HD DY DRM CW SML. Contributed reagents/materials/analysis tools: NK. Wrote the paper: HD DRM SML.

References

- Lemon SM, Walker C, Alter MJ, Yi M (2007) Hepatitis C viruses. In: Knipe DM, Howley PM, Griffin DE, Martin MA, Lamb RA, et al., editors. *Fields Virology*, 5th Ed. Philadelphia: Lippincott Williams & Wilkins. pp. 1253–1304.
- Lemon SM (2010) Induction and evasion of innate antiviral responses by hepatitis C virus. *J Biol Chem* 285: 22741–22747.
- Yoneyama M, Kikuchi M, Natsumura T, Shinobu N, Imaizumi T, et al. (2004) The RNA helicase RIG-I has an essential function in double-stranded RNA-induced innate antiviral responses. *Nat Immunol* 5: 730–737.
- Wang N, Liang Y, Devaraj S, Wang J, Lemon SM, et al. (2009) Toll-like receptor 3 mediates establishment of an antiviral state against hepatitis C virus in hepatoma cells. *J Virol* 83: 9824–9834.
- Kato H, Takeuchi O, Sato S, Yoneyama M, Yamamoto M, et al. (2006) Differential roles of MDA5 and RIG-I helicases in the recognition of RNA viruses. *Nature* 441: 101–105.
- Alexopoulou L, Holt AC, Medzhitov R, Flavell RA (2001) Recognition of double-stranded RNA and activation of NF- κ B by Toll-like receptor 3. *Nature* 413: 732–738.
- Kawai T, Akira S (2011) Toll-like receptors and their crosstalk with other innate receptors in infection and immunity. *Immunity* 34: 637–650.
- Hornung V, Ellegast J, Kim S, Brzozka K, Jung A, et al. (2006) 5'-Triphosphate RNA is the ligand for RIG-I. *Science* 314: 994–997.
- Vercammen E, Staal J, Beyaert R (2008) Sensing of viral infection and activation of innate immunity by toll-like receptor 3. *Clin Microbiol Rev* 21: 13–25.
- Xagorari A, Chlichlia K (2008) Toll-like receptors and viruses: induction of innate antiviral immune responses. *Open Microbiol J* 2: 49–59.
- Johnsen IB, Nguyen TT, Ringdal M, Tryggestad AM, Bakke O, et al. (2006) Toll-like receptor 3 associates with c-Src tyrosine kinase on endosomes to initiate antiviral signaling. *EMBO J* 25: 3335–3346.
- de Bouteiller O, Merck E, Hasan UA, Hubac S, Benguigui B, et al. (2005) Recognition of double-stranded RNA by human toll-like receptor 3 and downstream receptor signaling requires multimerization and an acidic pH. *J Biol Chem* 280: 38133–38145.
- Saito T, Owen DM, Jiang F, Marcotrigiano J, Gale M, Jr. (2008) Innate immunity induced by composition-dependent RIG-I recognition of hepatitis C virus RNA. *Nature* 454: 523–527.
- Loo YM, Owen DM, Li K, Erickson AL, Johnson CL, et al. (2006) Viral and therapeutic control of interferon beta promoter stimulator 1 during hepatitis C virus infection. *Proc Natl Acad Sci USA* 103: 6001–6006.
- Meylan E, Curran J, Hofmann K, Moradpour D, Binder M, et al. (2005) Cardif is an adaptor protein in the RIG-I antiviral pathway and is targeted by hepatitis C virus. *Nature* 437: 1167–1172.
- Li XD, Sun L, Seth RB, Pineda G, Chen ZJ (2005) Hepatitis C virus protease NS3/4A cleaves mitochondrial antiviral signaling protein off the mitochondria to evade innate immunity. *Proc Natl Acad Sci USA* 102: 17717–17722.
- Li K, Chen Z, Kato N, Gale M, Jr., Lemon SM (2005) Distinct poly-I:C and virus-activated interferon signaling pathways in hepatocytes. *J Biol Chem* 280: 16739–16747.
- Li K, Foy E, Ferreon JC, Nakamura M, Ferreon ACM, et al. (2005) Immune evasion by hepatitis C virus NS3/4A protease-mediated cleavage of the TLR3 adaptor protein TRIF. *Proc Natl Acad Sci U S A* 102: 2992–2997.
- Targett-Adams P, Boulant S, McLauchlan J (2008) Visualization of double-stranded RNA in cells supporting hepatitis C virus RNA replication. *J Virol* 82: 2182–2195.
- Limmon GV, Arredouani M, McCann KL, Corn Minor RA, Kobzik L, et al. (2008) Scavenger receptor class-A is a novel cell surface receptor for double-stranded RNA. *FASEB J* 22: 159–167.
- Dieudonne A, Torres D, Blanchard S, Taront S, Jeannin P, et al. (2012) Scavenger receptors in human airway epithelial cells: role in response to double-stranded RNA. *PLoS One* 7: e41952.
- DeWitte-Orr SJ, Collins SE, Bauer CM, Bowdish DM, Mossman KL An accessory to the 'Trinity': SR-As are essential pathogen sensors of extracellular dsRNA, mediating entry and leading to subsequent type I IFN responses. *PLoS Pathog* 6: e1000829.
- Yamashita M, Chattopadhyay S, Fensterl V, Saikia P, Wetzel JL, et al. (2012) Epidermal growth factor receptor is essential for toll-like receptor 3 signaling. *Sci Signal* 5: ra50.
- Sarasin-Filipowicz M, Oakeley EJ, Duong FH, Christen V, Terracciano L, et al. (2008) Interferon signaling and treatment outcome in chronic hepatitis C. *Proc Natl Acad Sci U S A* 105: 7034–7039.
- Liang Y, Shilgard T, Xiao SY, Snyder N, Lau D, et al. (2009) Visualizing hepatitis C virus infections in human liver by two-photon microscopy. *Gastroenterology* 137: 1448–1458.